IMPROVEMENT OF OPTICAL AND PRESSURE SENSING CAPABILITIES OF THE UNC CHARLOTTE HYPERSONIC WIND TUNNEL

by

Michael White

A thesis submitted to the faculty of
The University of North Carolina at Charlotte
in partial fulfillment of the requirements
for the degree of Master of Science in
Mechanical Engineering

Charlotte

2021

Approved by:

_____
Dr. Peter Tkacik

_____
Dr. Jerry Dahlberg

_____
Dr. Russ Keanini

ABSTRACT

MICHAEL WHITE. Improvement of Optical and Pressure sensing capabilities of the UNC Charlotte Hypersonic Wind Tunnel. (Under the direction of DR. PETER TKACIK)

The UNC Charlotte hypersonic wind tunnel was designed and made by a team of engineering students in 2019. The wind tunnel is capable of holding 1500 PSI and sending air through a test chamber with viewing windows at Mach 3 and 5. The construction of the wind tunnel and confirmation of the wind tunnelâs performance were great feats achieved by the Hypersonic Senior Design team but further sensing capabilities on the wind tunnel are essential to the usefulness of the wind tunnel as a learning and research tool. A z-type schlieren system that uses refraction of light to view relative pressure differences through the center of the viewing window on the test chamber has been designed, fabricated and tested. This optical, qualitative measurement system will allow students and researchers to visualize boundary layer phenomena that occur around models under Mach 3 and 5 wind speeds. A linear actuated pressure sensing system that utilizes a pitot tube and pressure transmitters has been designed to be secured to the sidewall of the test chamber. This pressure sensing system sweeps a pitot tube back and forth through the center of the air flow in the test chamber providing continuous static and dynamic pressure readings during wind tunnel operation. The pressure sensing system provides the user with crucial information on the wind tunnelâs flow uniformity across the cross-section of the air flow as well as the true diameter of air flow traveling through the test chamber. The testing of the schlieren system has displayed phenomenal results as a stand-alone optical system and some room for improvement as an imaging system while the wind tunnel is operational. The testing with the pressure sensing system has shown quality measurement results, however the support system has proven to interrupt the flow through the test chamber. These sensing capabilities will, if nothing else, expose

students to high-level wind tunnel observation providing them with experiences they can use in the real world; however, both can be used in the hypersonic field of research as they stand.

DEDICATION

This Masters thesis is dedicated to my family. My father and mother, Jeffrey and Donna White, and my big sister Brittany Fry. There are no other people more deserving of the dedication of my masters thesis as they are the ones that made me who I am today. My parents provided me with amazing guidance and unwavering support throughout my life and cemented every lesson they taught me by leading by example. That allowed me to hear what I needed to hear but more importantly, see what I needed to see from the very beginning of my life to the present. My sister watched over me, helped take care and helped teach me throughout my life and I canât thank her enough for that. She, as the oldest child, led the path for me and indirectly showed me what hard work is while she pursued her Degree in Biology and continued by earning multiple advanced degrees in the medical field. I will forever be grateful for them and their influence on me.

ACKNOWLEDGEMENTS

I would like to express my deep gratitude to Dr. Peter Tkacik for his continuous guidance and support throughout my research as well as acting as my professor, advisor and mentor throughout my research experience. I would also like to thank Dr. Jerry Dahlberg and Dr. Russel Keanini for serving in my thesis committee and always being available to help me throughout my years in the research program. I would also like to thank Jason Solomon for working on improving the hypersonic wind tunnel with me. Another peer of mine, Michael Stokes, thanks for helping me understand the finer details of hypersonics and aiding me in some day-to-day tasks throughout my whole research process.

My gratitude also extends to the skilled machinists and lab managers at UNC Charlotte, Brian Dutterer, and Jim Fox for machining parts that I could not complete on my own. I also wish to thank Phillip Davis and Adam Stall for utilizing their welding skills to help further my research. Lastly, I would like to thank an old professor of mine, Dr. Jimmie Miller for sharing some of his expertise in the world of optical metrology in a way that helped the development of the schlieren system in its early stages.

TABLE OF CONTENTS

LIST OF TABLES

LIST OF FIGURES

LIST OF ABBREVIATIONS

BOS Background Oriented Schlieren

CCS Calibrated Color Schlieren

CFD Computational Fluid Dynamics

Mach Number Ratio of an object's speed to speed of sound

NPT National Pipe Threads - a US standard for tapered threads

PLC Programmable Logic Controller

UNCC University of North Carolina at Charlotte

CHAPTER 1: INTRODUCTION

1.1 UNCC Hypersonic Wind Tunnel

The hypersonic wind tunnel at the University of North Carolina at Charlotte was designed and built by a team of students the fall and spring semesters of the 2019 school year. The purpose of the Hypersonic Wind Tunnel is create Hypersonic Researchers at UNC Charlotte by giving them the opportunity to work with the tools required to find solutions to the problems in the field of hypersonics. The Hypersonic Wind Tunnel Team was led by Jason Solomon and mentored by Dr. Peter Tkacik and Dr. Jerry Dahlberg. The wind tunnel is comprised of five major subsystems, each led by an individual team member. The Air Storage subsystem was led by Christian Struckmeyer; the Heater was led by Michael Allen; the Hypersonic Nozzles were led by Jason Solomon; the Test Chamber was led by myself and the Diffuser/Silencer subsystem was led by Rollins Stewart.

1.2 Theory

1.2.1 Manifold

The critical component of the manifold is the part of the manifold that will feel the highest internal pressure. That means that the center tube that runs across the length of the hypersonic wind tunnel is the critical component because it is the longest pipe with the largest diameter. the cross section can be modeled as a tube shaped vessel experiencing hoop stress that can be calculated using Equation (1.1).

$$\sigma_{hoop} = \frac{Pd}{2t} \tag{1.1}$$

where:

σ_{hoop} = hoop stress

P = internal pressure

d = diameter of the pipe

t = wall thickness

The center tube can also be modelled by a tube with 2 closed ends. Stress along the axis of the cylinder can be calculated using Equation (1.2) but this is not a critical calculation since hoop stress will be a source of failure in the pipe before axial stress will.

$$\sigma_{axial} = \frac{Pd}{4t} \tag{1.2}$$

where:

σ_{axial} = axial stress

P = internal pressure

d = diameter of pipe

t = wall thickness

After the hoop stress is calculated, it is determined to be the maximum stress felt by the manifold. the yield stress of the A36 steel used in the manifold is 36,300 PSI. The Factor of Safety of the manifold is then calculated using Equation (1.3).

$$FOS = \frac{s_y}{\sigma_{max}} \tag{1.3}$$

where:

s_y = yield stress of A36 steel

σ_{max} = maximum stress felt by center pipe

Table 1.1 displays the input data and calculation results used to justify the manifold build. A factor of safety of 2.3 using 3000 PSI as the internal pressure (which is 600 PSI higher than the expected operating pressure) proves that the pipes and fittings chosen for the manifold are safe.

Table 1.1: Manifold Justification Inputs and Calculations

Nominal diameter	1.5	inches
Wall thickness	0.12	inches
Inner diameter	1.26	inches
Internal Pressure	3000	PSI
σ_{hoop}	15,750	PSI
FOS	2.3	N/A

1.2.2 Heater

The heater, which is designed to transfer electrical energy as heat to high pressure, fast moving air before the air is choked at the nozzle. More specifically, the air entering the nozzle must be heated to 300 degrees Celsius in order to prevent liquefaction. Equation (1.4) is used to identify how hot the heating elements must get to heat the air to the desired value.

$$\frac{\pi D^2}{4}\rho C_p\frac{\Delta T}{\Delta t} = -FC_p\frac{\Delta T}{\Delta x}\Delta t + U\pi D(T_a - T(x,t)) \tag{1.4}$$

where:

T_a = Heater Temperature

U = heat transfer coefficient of heating element

D = pipe diameter

ρ = inlet air density

C_p = specific heat capacity of air

F = mass flow rate of air

T_o = inlet air temperature

ΔT = time step

Δx = distance step

In order to identify if the heater design can be reasonably achieved the energy required to heat the air to the desired temperature must be identified. This value depends heavily on the properties of the heating elements being used. First the time available to heat the air is calculated using Equation (1.5). Then the energy required to heat the amount, or mass, of air that will exist inside each heating element at any given time is calculated using Equation (1.6). Finally, the power required to be supplied to the heater can be calculated using Equation (1.7).

$$\Delta t = \frac{L}{v} \tag{1.5}$$

where:

L = length of the pipe

v = velocity of the air traveling through the pipe

$$Q_{req} = mc\Delta T \tag{1.6}$$

where:

c = specific heat capacity of air

m = mass of air

ΔT = temperature change

$$P_{req} = \frac{Q_{req}}{\Delta t} \tag{1.7}$$

1.2.3 Nozzle

Before being fabricated two very critical values considering the Nozzles must be identified. First, the area ratio between the exit of the De Laval nozzle and the choke point must be calculated so that a reasonable exit area can be chosen, then a choke point area value can be calculated. Second, the required pressure upstream of the nozzle must be calculated depending heavily on the pressure downstream of the nozzle.

$$\frac{A_e}{A^*} = (\frac{\gamma+1}{2})^{-\frac{\gamma+1}{2(\gamma-1)}} \frac{(1+\frac{\gamma-1}{2}M^2)^{\frac{\gamma+1}{2(\gamma-1)}}}{M} \tag{1.8}$$

where:

A_e = exit area

A^* = throat area

γ = specific heat ratio

M = desired Mach number

$$\frac{P_e}{P_t} = (1+\frac{\gamma-1}{2}M_e^2)^{-\frac{\gamma}{\gamma-1}} \tag{1.9}$$

where:

P_e = exit/downstream pressure

P^t = inlet/upstream pressure

γ = specific heat ratio

M = desired Mach number

Note that Equation (1.8) and (1.9) are both functions of the desired Mach number. So, assuming a constant exit area for each nozzle and downstream pressure, calculations for throat area and upstream pressure must be calculated for each desired Mach

number. Table 1.2 below displays all of the caclulated values for each desired Mach number that the UNCC Hypersonic Wind tunnel has been designed to achieve.

Table 1.2: Throat Area and Upstream Pressure values for each Desired Mach Number with a constant Exit Area of 7854 mm^2 and Downstream Pressure of 14.7 PSI

Mach Number	A^*
3	1848 mm^2
5	291 mm^2
7	76 mm^2

1.2.4 Test Chamber

In order to safely allow hypersonic flow to pass through the test chamber the chamber must have an inlet and outlet for the flow to travel through and most importantly, the chamber must neither explode, nor collapse under the pressure it will feel from the flow itself. This seems quite obvious. With the design of the test chamber, three components have the potential of failure. The three ways the test chamber could fail are breaking of the viewing windows, excessive deflection of the sidewalls and having the bolts keeping the chamber together explode out of their threads. In order to confirm the test chamber sidewalls would not deflect excessively, the sidewalls were modeled as very wide beams secured on each end. A maximum acceptable deflection was determined so that required thicknesses of different materials could be calculated using Equation (1.10) below.

$$\delta(x) = \frac{\omega x^2}{24EI}(l - x)^2 \tag{1.10}$$

Knowing that the maximum deflection of a beam under a load that is equal across the beam occurs at the center of the beam, Equation (1.11) can also be used to find required thickness.

$$\delta = \frac{\omega l^4}{384EI} \tag{1.11}$$

where:

δ = deflection

ω = distributed force across the sidewall

l = length of the sidewall

E = modulus of elasticity of sidewall material

I = inertia of sidewall according to thickness

x = position across length of sidewall

To ensure that the bolts holding the test chamber together would have enough strength to hold the test chamber together, calculate the bolt pull out force of bolts of different available sizes. The amount of force felt by sidewall due to the internal pressure would be divided by the number of bolts used to hold the sidewalls in place. That value needed to be less than that of the value calculated using Equation (1.12) below.

$$F = S_s A = S_s \pi D_p L = \frac{S_t}{\sqrt{3}} \pi D_p L \tag{1.12}$$

where:

F = bolt pull out force

S_s = shear stress

S_t = tensile yield stress

A = shear area

D_p = pitch diameter

L = axial length of full thread engagement

1.2.5 Diffuser

1.2.6 Wind Tunnel Design and Objectives

Much of the design considerations and objectives of the UNC Charlotte hypersonic wind tunnel can be found in a thesis written by Jason Solomon titled, "The Design, Calibration, and Commissioning of a Benchmark Hypersonic Wind Tunnel". [31]

1.2.6.1 Frame

The frame is designed to securely hold the air tanks and manifold in place while providing a straight line of assembly for the rest of the system using a Unistrut across the length of the table. To achieve this, 2 by 4-inch, eighth inch thick square pipes of various lengths were TIG welded together to create a frame that is 14 feet long by 4 feet wide and stands 4 feet tall. Six 6-foot-long slots were welded across the length of the frame on each end serving as places for the air tanks to fit without room to roll around. Pieces of butcher block were cut, treated and secured to the frame around two rows of Unistrut rods that run across the length of the table secured to the frame with 5/8 inch bolts.

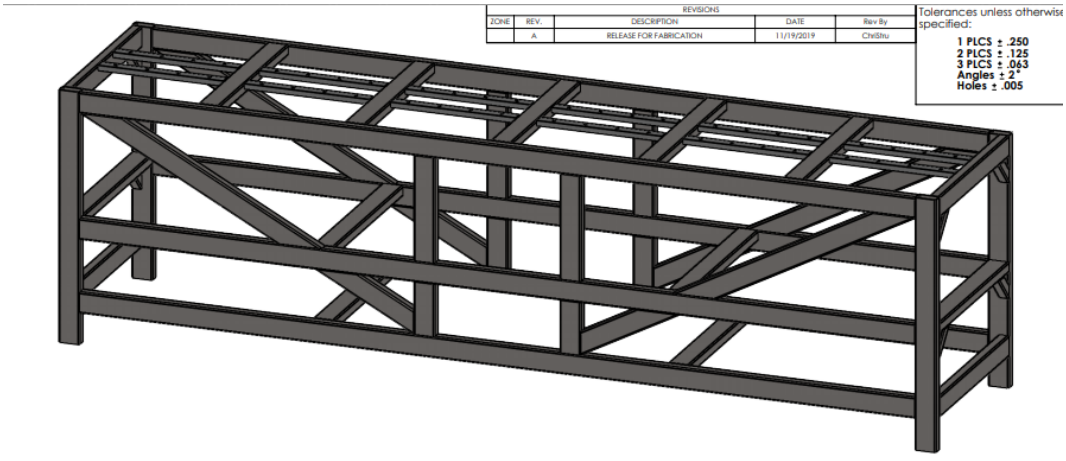

Figure 1.1: This is the CAD Model of the Frame supporting all components of the UNCC Hypersonic Wind Tunnel

1.2.6.2 Manifold

The manifold is designed to accept pressurized air from a compressor, hold the compressed air at 2400 PSI and provide compressed air to the rest of the system when called to do so. The magnitude of the pressure of the air stored in the manifold determines the upstream to downstream pressure ratio, which is significant to the value of the Mach number produced behind the choke of the nozzle. The volume of the condensed air in the manifold determines how long the desired Mach number can be sustained for.

Two primary designs to this subsystem already exist in the industry. One of the designs is to use a large volume tank as the air storage system. The advantage of a large volume air storage system is the simplicity in design with almost no losses in pressure when providing the stored air to the rest of the system. The primary disadvantage of this method is the cost of such a large volume tank that is rated to hold the high pressure required. The other design uses multiple air tanks connected to each other and the rest of the tunnel with a piping system that is secured to the frame. The advantages of the second design are cost and freedom to arrange the tanks in an efficient way within the frame. The disadvantages are complexity of design and fabrication as well as higher losses of pressure when the air is being provided to the system due to all the 90 degree turns the flow must take before reaching the system. [32]

With the budget in mind, the Senior Design team chose the air storage system that utilized tanks and a pipe system in its manifold. First, a piping system was designed to fit inside the frame and connect twelve 4 and a half feet long tanks with a 9-inch diameter to each other and the rest of the system. The piping system was built using Schedule 160 pipes and fittings, which are rated to hold 3000 PSI, acquired from McMaster Carr. The air tanks were depressurized and the valves provided by the manufacturer were removed so that 1 foot long flexible fittings could be used

to attach each tank to its respective fitting in the pipe system. The pipe system uses two crosses, three unions, twelve t-fittings and eight elbow fittings to connect almost 30 collective feet of straight pipe. Most of the straight pipe was bought from and tapped by the manufacturer but some of the straight pipes had to be cut and threaded using an NPT die. It is important to note that when threading the straight pipes, it is important not to thread too far down the length of the pipe as that could cause part of the thread to be straight instead of tapered which will cause a misfit between the thread of the straight pipe and the tap of a fitting. Also, when tapping a hole, it is important to back up the tap while cutting the material to break off chips and get a clean cut, but when threading pipes, the die must not be backed out to break chips because that could roll the thread metal. Instead, thread the end of the straight pipes in just one go and only back out when the thread is finished. Once the straight pipes are all cut to length and threaded, they are assembled using low locking strength Loctite that is rated to hold 10,000 PSI between any and all joints and a 3-foot pipe wrench. The piping system connects all the tanks to each other using two U-shaped assemblies that combine to each other at a cross. The cross then directs the pressurized air upward to the bottom of the top-surface of the frame and then the air directed from the middle of the frame towards the front end of the frame using a series of elbow fittings. Then, for safety, a manually actuated valve rated to hold 10,000 psi is assembled between two straight pipes before two more elbow fittings direct the air out from under the table pointed towards the back end of the table parallel to the length of frame.

The final component of the Manifold is the Bonomi 8P3002 pressure actuated Fast Valve rated to hold 4500 PSI. This fast valve is held in a normally closed position as is the final stopping point of the pressurized air before being released from the manifold to the rest of the system. It is powered by shop air that flows at 100 PSI and

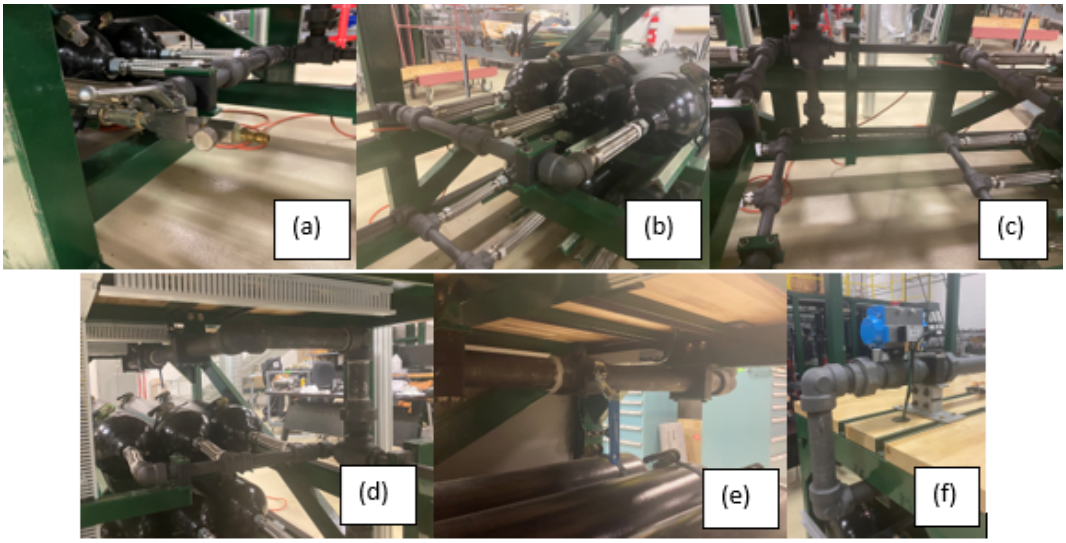

Figure 1.2: This figure displays the key components of the manifold. The image denoted by (a) displays the male fitting to a ball valve connected to a manual valve rated to 10,000 PSI. (b) denotes a visual of the connections made between the high pressure tanks to the rest of the manifold with flexible tubing. (c) displays the double-u arrangement of the manifold connecting all tanks to one central system. (d) shows how the air is directed to the center and then down the length of the frame of the hypersonic wind tunnel. (e) is an image of a manual valve in between the high pressure system and the fast valve while (f) shows a picture of the piping that re-directs the airflow upward and then back in the direction that it came from

actuated with a PLC program that uses ladder logic to connect a push button to the fast valve controlling its open and closed state with an actuation speed of 0.25 seconds.

1.2.6.3 Heater

One of many challenges of a properly operational hypersonic wind tunnel is the problem of liquefaction. When the already compressed air from the manifold travels through the choke point of the nozzle the pressure increases so much that the pressure and temperature increase dramatically causing some of the air to liquefy and get sent through the exit of the nozzle in a liquid state instead of the desired gaseous state. To prevent this from happening the upstream flow must be heated before entering the nozzle. Two primary solutions to this problem already exist. The first is to heat up the air in the manifold [6] and the second is to heat the air upstream of the nozzle as

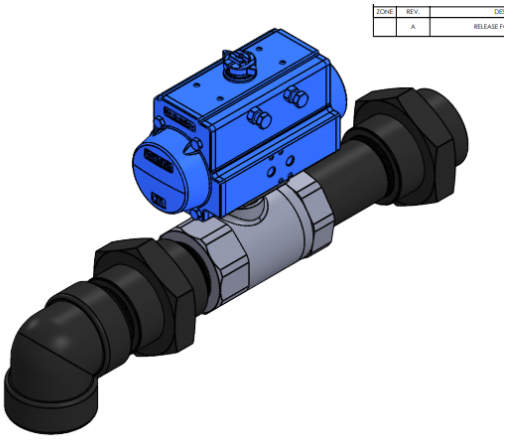

Figure 1.3: This is the CAD Model of the Bonomi 8P3002 Fast Valve

it travels through the system[12]. Heating the air in the manifold is a simpler method of heating the air but causes the pressure ratings of the straight pipes and fittings to be less reliable so storing this high volume of heated and compressed air becomes much more difficult and unsafe. So, for this hypersonic wind tunnel a heater will be placed in between the fast valve and the inlet of the nozzle. To heat up the air the flow stream must be broken up from one large flow stream to multiple smaller flow streams to increase the amount of air that contacts the heating elements.

The hypersonic wind tunnel at Virginia Tech uses a heater that splits up the primary flow stream into 8 smaller flow streams that travel through ceramic pipes that are heated up using a power source of about 15 mega watts in order to provide the air with enough energy to heat it up to a sufficient temperature of 300 degrees Celsius.

The optimal design for the heater features a 2 inch inlet that opens the flow up into a 8 inch diameter cavity where the primary flow steam splits into 12 different smaller flow streams that travel through 24 inch long ceramic pipes. Once the air travels through the ceramic pipes each flow stream is joined back together in the back end of the heater and directed out of the back end of the heater through a 2 inch hole.

Many calculations and designs were considered when trying to implement a heater

onto the UNCC hypersonic wind tunnel. Unfortunately, the best design was too expensive for the Senior Design team to implement. All designs that fit the budget were considered to have insufficient methods of heating or had too high of a potential to damage the downstream components of the wind tunnel, particularly the expensive and time-consuming nozzles directly behind the heater. If any heating components ended up damaging inner profile of the nozzle the whole wind tunnel would be inoperational so the team decided not to test different methods with the objective of ensuring the safety of the highly critical nozzles. Instead, a mock heater is designed from steel in a way that would imitate how the airflow would be directed into the inlet of the nozzle. This way, the system could be operational without a heater up to Mach 5 or 6 until a legitimate and safe heater could be fabricated.

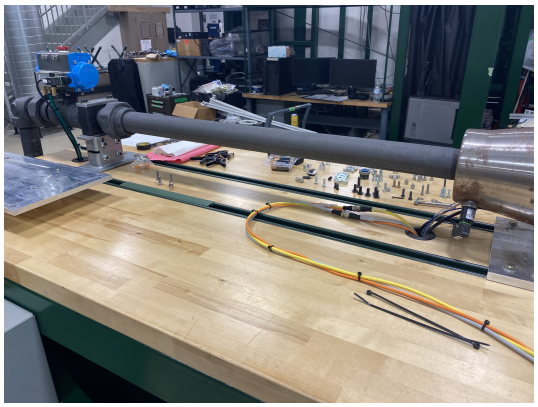

Figure 1.4: The Mock Heater being used in place of the real heater

1.2.6.4 Nozzles

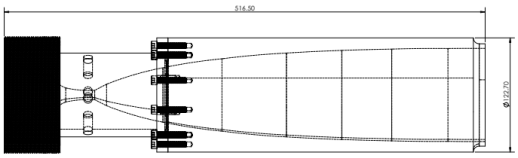

Figure 1.5: Skeleton View of Mach 5 Heater

The nozzles used in hypersonic wind tunnels speed up air flow using the principle

of conservation of matter and first designed by De Laval. The flow of air entering the nozzle is choked, limiting the amount of air that can exit the nozzle. Therefore, less air can exit the nozzle than is entering however, the mass flow rate must be the same on each end of the choke. So, since the volume of the air leaving the nozzle is less than the volume of air entering the nozzle at any give time, the velocity of the air exiting the nozzle must be higher than the air entering the nozzle. This principle leads to the derivation of two significant equations used to determine the Mach number of the air exiting the nozzle. The pressure ratio, which considers the pressure of the air upstream of the nozzle and the pressure of the area downstream of the nozzle and the area ratio, which considers the ratio of the area of the choke point of the nozzle and the area of the exit of the nozzle. The principle equations used to design the nozzles are further described in the methodology chapter of this paper.

The pressure ratio determines the pressure required to be built up in the manifold according to the desired Mach number while the area ratio determines the dimensions of the inner profile of the nozzle. The area ratio is fairly simple to follow when designing the nozzle. First the expected exit area is determined according to the desired flow of air at hypersonic speeds, then the desired Mach number is chosen and the area of the choke can be determined. With that being said, a different nozzle is required for each desired Mach number. The dimensions of the exit area and choke area for each desired Mach number are displayed in Table 1.3 below.

Table 1.3: Mach Number and Nozzle Dimension Values

Mach Number	Choke Area	Inlet Area	Area Ratio
3	1848 mm^2	7854 mm^2	4.25
5	291 mm^2	7854 mm^2	26.99
7	76 mm^2	7854 mm^2	103.34

The pressure ratio value is subject to the design of the wind tunnel itself. For example, some wind tunnels blow air from the manifold into a vacuum. This would require an isolated air storage system with a huge volume as well as a compressor

that could pull air from the air storage system before every test to create a vacuum effect downstream of the nozzle. This method had plenty of advantages, as it requires a much lower upstream pressure value stored in the manifold. However, the cost and space requirements of such a vacuum system were way too high for the budget of the Senior Design team. So, the hypersonic wind tunnel at UNCC blows air from the manifold into the atmosphere which as a pressure of about 14.7 PSI plus or minus up to one PSI depending on the weather that day.

The dimensions of the inner profile of the nozzles were very important, but a proper method of securing the nozzles to the rest of the system is just as important. So, the nozzle was designed to be threaded in to the back of the heater. The back end of the eater is designed to accept those threads while directing the air into the nozzle in an uninterrupted. The exit of the nozzle features a tapered tip that fits snugly into the entrance of the test chamber in a way that allows the flow of air to travel uninterrupted into the test chamber.

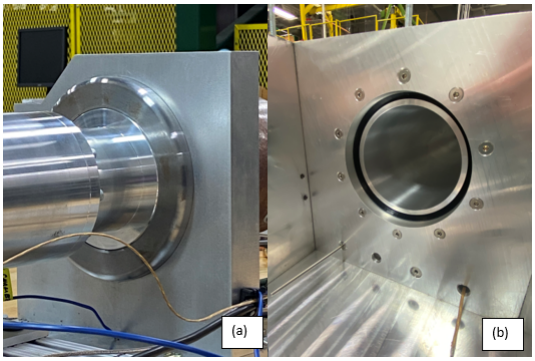

Figure 1.6: This figure displays the (a) the nozzle tapped into the back end of the mock heater and (b) a smooth fit of the exit of the Nozzle into the entrance of Test Chamber

1.2.6.5 Test Chamber

The test chamber was designed to provide a safe and observable region for air to travel through at hypersonic speeds. The key features to this design are the 6-inch

viewing windows mounted to the side walls of the test chamber that will allow models to be observed using a schlieren system that uses 4-inch mirrors. Another key feature is the 3D printed inlet mount bolted to the inlet hole of the test chamber. This inlet mount matches the tapered tip on the nozzle which allows the nozzle to slide snugly into the test chamber and provides no sharp edges for the flow to get caught on before traveling through the center of the test chamber. The last key feature of the test chamber is the bell-shaped outlet hole machined into the backwall of the test chamber. This feature is included to ensure that all the flow entering the test chamber exits fluently even if it expands a little bit after entry.

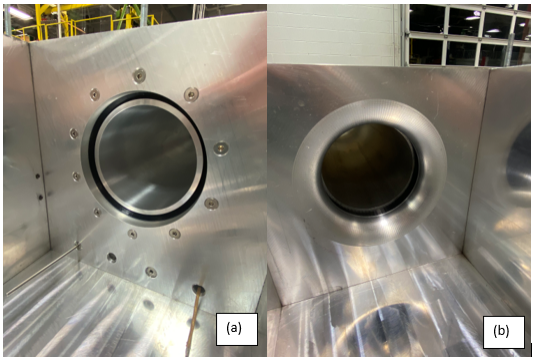

Figure 1.7: This figure displays the (a) smooth fit of the exit of the Nozzle into the entrance of Test Chamber and (b) the bell curve machined around the exit hole of the Test Chamber

The test chamber itself is composed of two half inch sidewalls bolted to a half inch front wall, a 1-inch thick backwall and a 1-inch thick base. All of these walls are bolted together securely with 0.25 inch -20 bolts. The top surfaces of both sidewalls, the front wall and the back wall have 0.25 inch-20 tapped holes that fit threaded rods in them. The pattern of those holes match the pattern of 0.26 inch clearance holes drilled in the half inch thick lid which allows the lid to be secured on to the rest of the test chamber with fly nuts as an easy attachment and removal process. The easy removal of the lid is important because the stinger, which holds all models that are to

be tested in the wind tunnel, will be secured to the lid with M6 bolts near the back end of the length of the test chamber. Easy removal and attachment of the lid means easy removal and attachment of different test models. The test chamber is secured to the frame of the wind tunnel at the base with 5/8 inch bolts and t-nuts that fit in the Unistrut.

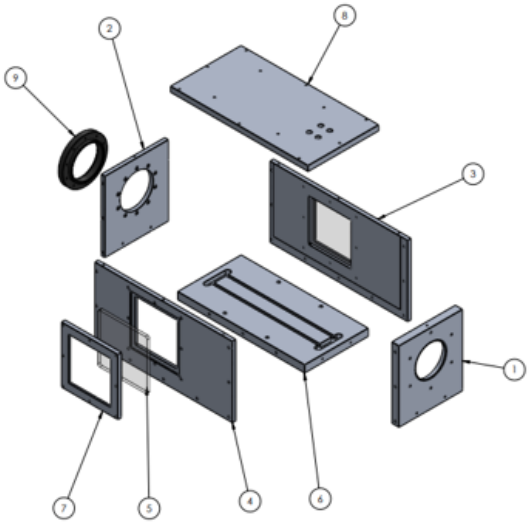

ITEM NO.	PART NUMBER	DESCRIPTION	QTY.
1	60001	BACK WALL	1
2	60005	FRONT WALL	1
3	60002	LEFT SIDE WALL	1
4	60003	RIGHT SIDE WALL	1
5	60004	SIDE WALL WINDOW	2
6	60013	CHAMBER BASE PLATE	1
7	60014	WINDOW FRAME	2
8	60015	CHAMBER LID	1
9	60016	NOZZLE ADAPTER RING	1

Figure 1.8: This is the exploded view of the Test Chamber with each of its components labeled and listed

1.2.6.6 Diffuser

The initial purpose of the diffuser was to provide the hypersonic flow with a directional pipe that expands at a slight angle. This expansion allows the flow itself to expand and slow down before exiting in to the atmosphere.

After a few tests it became aparent that the diffuser is critical to achieving hypersonic flow through the test chamber. Instead of just providing a smooth exit for the flow, the diffuser actually swallows the shock of the flow that would inhibit flow if it immediately exited to the atmosphere. When the diffuser swallows the shock from the flow, it pulls the flow from the test chamber through the diffuser causing a vacuum

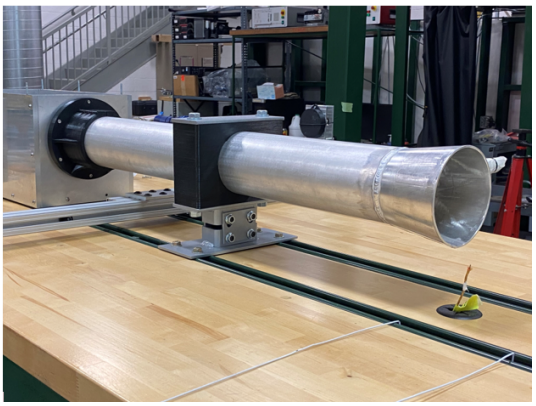

Figure 1.9: This is a picture of the Diffuser that is used with the Mach 5 Nozzle assembled secured to the back end of the Test Chamber

effect in the test chamber which allows the pressure ratio between flow upstream and downstream from the nozzle to be maximized. The calculations determining the exact dimensions and angle of expansion of the diffuser are explained more thoroughly in the methodology chapter.

1.2.6.7 Silencer

The wind tunnel blows air that starts at 2400 PSI into the atmosphere at hypersonic speeds so, naturally it is a very loud machine. Anyone operating or in the area of operation of the wind tunnel must wear high quality sound-reducing earphones. In order to reduce the sound of the wind tunnel a silencer is placed at the end of the diffuser. The silencer is a box of steel sheet metal welded together with perforated sheet metal welded together in the shape of a triangle when observing from the top view. A sharp knife edge is welded on where the two perforated sheets meet each other. The knife edge splits the exit flow into tow distinct flow paths and then the holes in the perforated sheet metal spit flow into even smaller flow paths. This action distinctly reduces the sound of the wind tunnel during operation which improves the audible safety of the system as a whole.

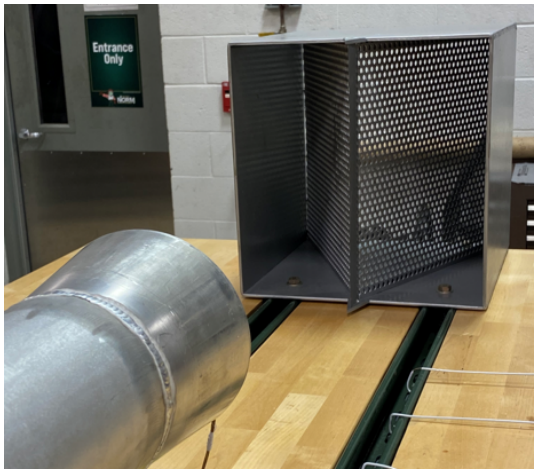

Figure 1.10: This is an image of the Silencer secured to the Wind Tunnel with locking nuts made for the uni strut

1.2.7 Wind Tunnel Sensing

1.2.7.1 Manifold

In order to ensure that the compressor has pumped the manifold up to the required pressure value of 2400 PSI a pressure gauge is threaded into the manifold. This pressure value represents the required stored pressure calculated by the pressure ratio explained in the Nozzle section.

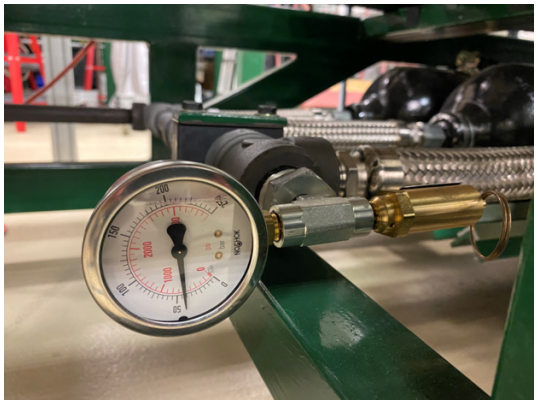

Figure 1.11: This is an image of the pressure gauge tapped into the Manifold

1.2.7.2 Heater

To transfer enough heat from the heater to the air upstream of the nozzle, a thermocouple attached to each ceramic tube is required. These thermocouple values will inform the user whether or not the heater is hot enough for operation at Mach speeds greater than 5.

A thermocouple tapped into the back end of the heater will be used to measure the air temperature during operation of the hypersonic wind tunnel. This thermocouple value with allow the user to identify if the heater is working properly. A low reading at this point will show that there is not enough heat transfer occurring between the ceramic tubes and the flow while a high reading will show that the ceramic tubes were heated up too much before testing.

A pressure transmitter at the inlet as well as the outlet of the heater will provide quality data for any run where the heater is required to be on. The pressure transmitter tapped into the heater near its inlet will allow the user to identify how much losses occur from the air traveling through the piping system. The pressure transmitter tapped into the heater near the outlet will inform the user the pressure differences that occur due to the heating of the air. Since air should be travelling pretty quickly through the heater there is not an expected difference in pressure between the air at the inlet and the outlet of the heater but any pressure difference at all will affect calculations and results of data. If the hypersonic wind tunnel is operational without the need of heater use, only one of the pressure transmitters tapped into the heater would be required. Ideally, the transmitter closer to the outlet will be used since that will most accurately give a value of the pressure value upstream of the nozzle.

1.2.7.3 Nozzles

The inner profile of the nozzles is very sensitive and accurately dimensioned. So, in order to preserve the integrity of the nozzles no sensors will be tapped into this component. Instead sensors inside the heater and test chamber will provide data for pressure upstream and downstream from the nozzle.

1.2.7.4 Test Chamber

A pressure transmitter rated to measure -14.7-30 PSI is tapped into the front face of the test chamber below the back end of the nozzle. Before wind tunnel operation this measurement will provide the user with the exact pressure reading downstream of the nozzle, which is ambient pressure. During operation of the wind tunnel this pressure transmitter will measure the pressure of the test chamber itself around the hypersonic flow. This measurement will help confirm proper operation of the wind tunnel and that an adequate seal of the test chamber from the outside environment exists.

A thermocouple with the ability to measure temperature data is tapped into the front face of the test chamber. This data serves its purpose by providing the user with the temperature change around the air flow caused by the hypersonic speed of the air flow traveling through the center of the test chamber.

1.2.7.5 Diffuser

By the time the air flow has reached the diffuser all the required sensing data has pretty much been taken. There could be a thermocouple used to confirm the temperature of the flow is normalized but, as long as the air flow travels uninterrupted through the test chamber that data is not extremely useful.

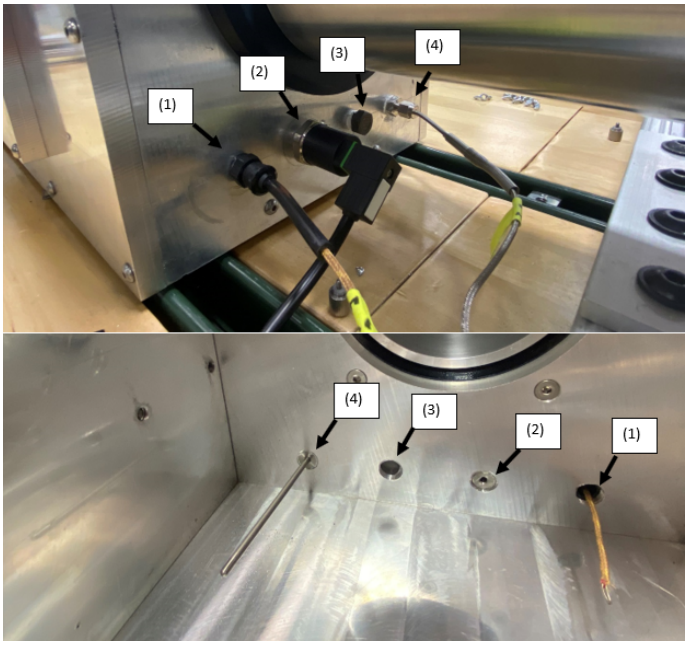

Figure 1.12: This figure displays the sensors measuring temperature and pressure along with their respective locations on the front wall of the Test Chamber. Sensor (1) is a thermocouple capable of measuring temperature values. Sensor (2) is a Pressure transmitter that measures pressure values between -14.7 and 30 PSI. The number (3) indicates a 1/4"-20 tap available for any sensor that can thread into the tap. Sensor (4) is a thermocouple capable of measuring temperature.

1.2.7.6 Silencer

In order to prove the usefulness of the silencer an audio recording of the wind tunnel should be taken at the location of the silencer that measured the number of decibels emitted by the wind tunnel. An audio recording taken without the silencer first and then with the silencer secured to the Unistrut would provide insightful data about the usefulness of the silencer.

1.2.8 Wind Tunnel Controls and Programming

The controls and programming of the hypersonic wind tunnel can be broken up into two distinct sections. The data collection portion and the operational portion. Both portions are wired to and powered through the control box secured to the frame

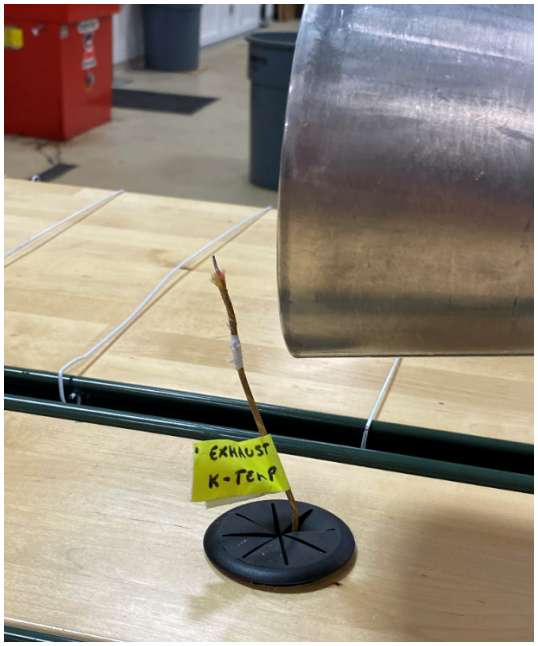

Figure 1.13: This figure is an image of the thermocouple that emerges from under the surface of the hypersonic wind tunnel close to and downstream of the diffuser

of the wind tunnel.

Figure 1.14: This figure displays the control box secured to the frame of the UNC Charlotte wind tunnel

1.2.8.1 Data Collection

The data collection system is powered by a LabView program written by the senior design team that can be easily added to as new sensors are added to the system. The sensors are wired through conduit in the frame of the wind tunnel to a National

Instruments SCXI. The LabView program features a DAQ assistant block which simply reads all of the data received by the analog inputs of the SCXI and displays the data to respective waveform charts. Once program is stopped, the data received during wind tunnel operation is automatically written to a text file and saved in a specific folder on the computer. The block diagram and command window of the LabView program are displayed in Appendix D.

Figure 1.15: The SCXI sitting below the control box on the UNC Charlotte hypersonic wind tunnel

1.2.8.2 Wind Tunnel Operation

The wind tunnel operation is controlled by the PLC from Automation Direct, programmed with DirectSoft. The fast valve and the push buttons secured to the door of the control box are wired to different input and output variable positions in the PLC. Ladder logic is used to connect a push button with the fast valve, which is powered by shop air at 100PSI. The programming allows for the actuation of the fast valve by pressing and holding a push button on the control box.

1.3 Purpose of Study

In the field of hypersonics there are three major areas limiting performance. The first is the high enthalpy or rate of heat transfer between the air particles and the

Figure 1.16: PLC from Automation Direct

vehicle traveling at hypersonic speeds. The second is material selection, or in other words, finding materials with the right properties to endure the forces that come with traveling at hypersonic speeds while still being light enough to be propelled at such high speeds. The third is the shape and aerodynamic effects of the vehicles. The purpose of this study is to use the hypersonic wind tunnel in the Motorsports Research Lab at UNCC to study the grain boundary flow of test models with different geometries and surface patterns. The test models will be shaped similarly to the nose of potential hypersonic vehicles and different patterns or geometries will be machined into the surfaces of each test model. The controlled test model will have no surface pattern; it will feature a smooth surface. Results will be collected in the form of Schlieren Images using a Z-type schlieren system with a high-speed camera. An analysis of the results will provide us with the optimal size and frequency of different patterns or surface geometries on the test models.

CHAPTER 2: Schlieren System

2.1 Theory

2.1.1 Overview

Schlieren imaging is a qualitative data collection method that utilizes light refraction properties to visualize relative pressure gradients that would be invisible to the naked eye. Light, from a source, is refracted by directing it through optical lenses, with optimal geometry to enhance the effects of refraction, or bounced off of optical quality mirrors, that also enhance the effects of refraction. Once the light either passes through a lens or bounces of a mirror, it is directed to a camera that can record the data at the required frequency or frame rate. A crucial component of a schlieren system is the knife edge, which blocks half of the light at the focal point of the mirror or lens before the light reaches the camera. The impact of the knife edge is described more thoroughly is the mathematical explanation section below.

2.1.2 Types of Schlieren Systems

The use of lenses versus mirrors and the orientation of the components depends on the objectives and constraints of the research project the schlieren system is being used for. There are many orientations that the schlieren system components can be arranged in but three primary systems are commonly used in research. Those systems are the lens system, double-pass single-mirror system and the Z-type two-mirror system, pictured below in Figure 2.1. [15]

Each system has its own draw-backs and advantages. The lens system takes the components and maintains a straight line assembly with the viewing path directly between the two lenses. The major draw-back with this system is that the viewing

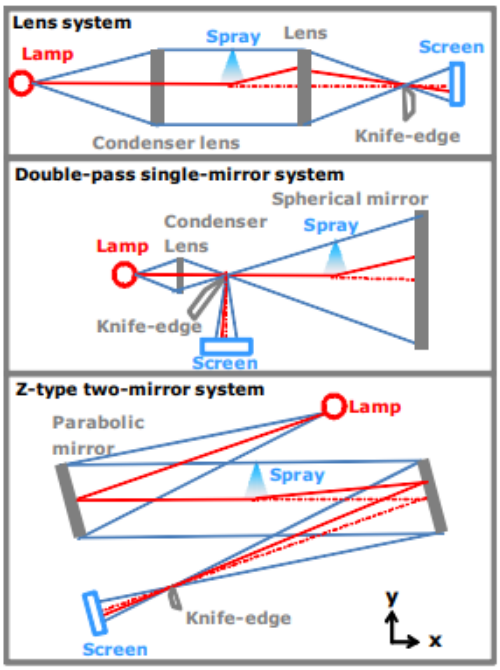

Figure 2.1: Schematic of the 3 most common types of Schlieren Systems used in research

field can only be as big as the diameter of the lenses used in the system. Since the price of lenses increases exponentially as diameter is increases, the system can get very pricey very quickly. So, if a large field of view is required for the research, the lens system is not ideal. The double-pass single-mirror schlieren system uses a spherical mirror to bounce light from a lamp to a viewing screen or camera. This system can keep costs minimal since only one spherical mirror is required and the condenser lens required is small since its purpose is to turn the lamp into a point source. However, the field of view of this system is limited to only a fraction of the diameter of the spherical mirror itself. So similarly to the lens system, if the field of view required for research is large, this system will not be cost effective. The Z-type double-mirror system bounces light from one spherical or parabolic mirror (both work), which collimates the light and directs it towards a second spherical or parabolic mirror. The second mirror directs the light past a knife edge and on to a viewing screen or into a camera. The Z-type schlieren system is the most popular

for multiple reasons. The viewing path is almost exactly as large as the diameter of the mirrors themselves. The distance between the lamp and the first mirror is a defining dimension and so is the distance between the second mirror and the knife edge, but the distance between the two mirrors can be very large. This makes the Z-type schlieren system ideal when research requires a viewing path through a test chamber that will not interfere with a preexisting machine or set up.

2.1.3 Common Errors in Schlieren Systems

Two common errors that exist in Schlieren Systems are comatic aberrations and astigmatism. Comatic aberrations are caused when the light source is off the mirror's optical axis. For an even better understanding of comatic aberrations, here is an excerpt from an article from Molecular Expressions by H. Ernst Keller that provides a clear example: "On a bright sunny day, use a magnifying glass to focus an image of the sun on the sidewalk and slightly tilt the glass with respect to the principle rays from the sun. The sun's image, when projected onto the concrete, will elongate into a comet-like shape that is characteristic of comatic aberration." [8] To fix comatic aberration, ensure that the light source is perfectly in line with the axis of the mirror or lens used in the schlieren system. Astigmatism is caused when the focusing point of the mirror or lens changes from the center along the radius of the mirror or lens. In other words, astigmatism occurs if the mirror or lens is made improperly and light focuses in different places depending on where it hits the mirror or lens. [14]

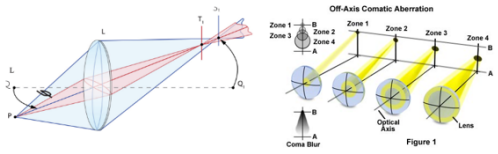

Figure 2.2: Visualization of comatic aberrations (on the right) and astigmatism (on the right)

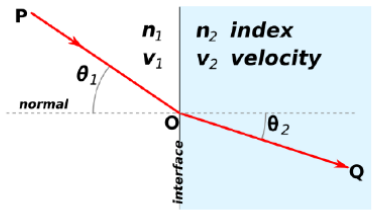

Figure 1: Refraction at the interface between two materials (Wikipedia)

Figure 2.3: 1 Beam Visualization of Snell's Law

2.1.4 Mathematical Explanation of Schlieren

The fundamental principle that makes schlieren imaging is Snell's law, also known as the law of refraction. This law states that refraction occurs because the speed of light changes when it passes into a new medium. The angle of refraction is a function of the refraction index change from one medium to another [16]. The visual of this phenomenon is displayed in Figure (2.3) and the equation that explains Snell's Law.

$$\frac{sin(\theta_1)}{sin(\theta_2)} = \frac{n_2}{n_1} \tag{2.1}$$

where: θ_1 = initial angle of light path

θ_2 = refracted angle of light path

n_1 = refractive index of medium 1

n_2 = refractive index of medium 2

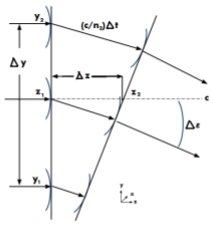

Figure 2: Diagram of light-ray deflection by a refractive-index gradient dn/dy

Figure 2.4: 2 Beam Visualization of Snell's Law

Figure (2.4) above shows Snell's Law with two different beams parallel to each

other and how they react with respect to each other while traveling through different mediums. This hold particular relevance to the schlieren system because the light in between two lenses or mirrors is collimated when properly aligned, meaning all of the light rays are parallel to each other. The geometric theory of refraction, states that the curvature of a refracted light ray is a function of the refractive index of the medium it travels through and considers this fact in two dimensions[21]. The equation that defines the geometric theory of refraction is displayed below.

$$\frac{\partial^2 y}{\partial x^2} = \frac{1}{n}\frac{\partial n}{\partial y} \tag{2.2}$$

As light travels through the test chamber over time period Δt, the light is refracted through a differential angle $\Delta\epsilon$ labeled in figure 2.4 above. This differential angle is calculated using the equation (2.2) below.

$$\Delta\epsilon = \frac{\left(\frac{c}{n_1} - \frac{c}{n_2}\right)}{\Delta y}\Delta t \tag{2.3}$$

we know that $\Delta t = \Delta z \frac{n}{c}$ so, substituting that into equation (2.3) gives us:

$$\Delta\epsilon = \frac{n}{n_1 n_2}\frac{(n_1 - n_2)}{\Delta y}\Delta z \tag{2.4}$$

If we assume that Δy is very small ($\Delta y approaches 0$), then we know $n \approx n_1 \approx n_2$ and we get the resulting equation.

$$\frac{d\epsilon}{dz} = \frac{1}{n}\frac{dn}{dy} \tag{2.5}$$

Then, the small angle approximation is used to postulate that $d\epsilon = \frac{dy}{dz}$ which gives us the integrateable equation (2.6).

$$\frac{\partial^2 y}{\partial z^2} = \frac{1}{n}\frac{\partial n}{\partial y} \tag{2.6}$$

Once integrated equation (2.6) provides the equations that allow for calculation or at least a mathematical understanding of the curvature of light rays that travel through optical homogenetities.

$$\epsilon_y = \frac{1}{n}\int \frac{\partial n}{\partial y}\partial z \tag{2.7}$$

$$\epsilon_x = \frac{1}{n}\int \frac{\partial n}{\partial x}\partial z \tag{2.8}$$

Equation (2.7) and (2.8) show how schlieren visualizes flows with a uniform refractive index gradient because of its knife edge. Some deflected rays are blocked while other deflected rays pass to the detector which causes a visualization in the phase differences.[15]

2.1.5 Factors Determining Schlieren Sensitivity

Understanding what components and variables are important to schlieren imaging is vital to being able to improve the system to be able to see the objective study. The relative change of image intensity can be given by equation (2.9). [25]

$$\frac{\Delta I}{I_o} = \frac{\delta}{d_F} = \frac{F_2\Theta}{d_F} = \frac{F_1\Delta\Theta}{d} \tag{2.9}$$

where: δ = deflection

F_1, F_2 = focal length of mirrors

ΔI = change in Intensity of the image

I_o = max possible intensity at completely open image

$d_F = \frac{F_2 d}{F_1}$ = width of light source image in a focal plane of a reception lens

d = width of light source

$\Delta\Theta$ = change in angle of any given light ray due to refraction

Using equation (2.9), the required minimum change in angle of any given light ray can be estimated mathematically. This value defines how sensitive the system will be by showing the minimum change in angle required while traveling from one medium through another. As shown in Figure 2.3 and Figure 2.4 if two mediums have similar indexes of refraction, the $\Delta\Theta$ value will be very little. Obviously, the system will be considered more sensitive if differences between mediums with similar indexes of refraction are distinctly visible. It is typically assumed that $\frac{\Delta I_m in}{I_o} \approx N^{-1}$ and in pretty much every schlieren system ever $F_1 = F_2 = F$. These assumptions applied to equation (2.9) help derive equation (2.10).

$$\Delta\Theta_{min} \approx \frac{d}{FN} \tag{2.10}$$

where: N = quantity of registered gray gradients (i.e. quality of camera

F = focal length of mirrors

d = the width of the light source

Looking at equation (2.10) it is easy to see that the size of the light source is the easiest variable to adjust when it comes to improving image sensitivity. More specifically, reducing the light source is the most efficient way to improve sensitivity of the schlieren system. [10] This is because the focal length of the mirrors are fixed according to the diameter of the mirrors which are typically chosen based on the desired viewing area and the quality of the camera is typically chosen based on budged allowance.

2.1.6 Recent Advancements

Schlieren imaging has been utilized regularly by researchers since about the 1960s as a qualitative data collection method. For a long time the improvements made to schlieren images have come from individual improvements of the schlieren system. Higher quality cameras led to higher quality images. Higher quality manufacturing methods led to higher quality lenses and mirrors, which led to more uniform and accurate manipulation of light rays. Recently, a lot of research has gone in to creating a schlieren system that can provide more quantitative data along with the qualitative data it provides naturally. Two methods have worked to achieve this goal better than any other. These methods are the calibrated color schlieren (CCS) and the background oriented schlieren (BOS). Both of these methods collect data in a way that provides the user with the projected density gradient in both spacial directions in the viewing plane. The density gradient vector field can be integrated using post processing methods to derive the projected density field. [24] CCS and BOS are comparable considering repeatably and accuracy of the data collected. However, BOS is more sensitive than CCS but BOS requires more prior knowledge of the flow field than CCS does to acquire the data.

2.2 UNCC Schlieren System

2.2.1 Components

2.2.1.1 Frame

The frame of the schlieren system is made of a collection of 1.5x1.5 inch and 1.5x3 inch 1018 Aluminum Extrusion. The frame consists of two separate assemblies, each designed to hold a Schlieren Mirrors in place along with a light source on one side and a high-speed camera on the other all at equal heights above the top surface of the wind tunnel. Each assembly secures the critical components to the frame using L-brackets bolted to the extrusion itself and the Unistrut running across the

length of the wind tunnel. With this frame design, the schlieren system can easily be assembled on to and removed from the hypersonic wind tunnel with just four bolts.

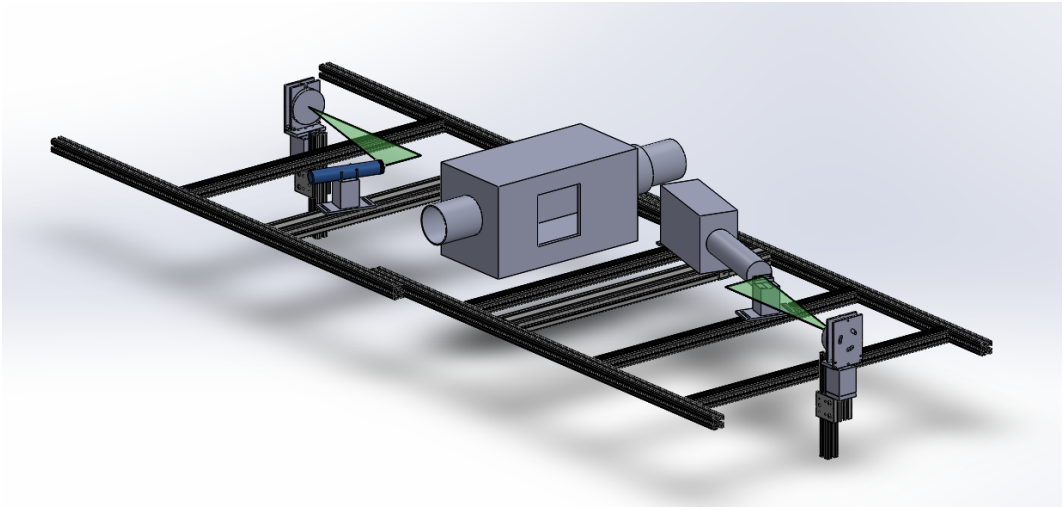

Figure 2.5: Full Schlieren Assembly

2.2.1.2 Light Source

The high-speed camera being used for the Schlieren system will be taking images at a very high rate of speed. An LED light source will not work, an incandescent light bulb is required. So, the incandescent bulb of a D-battery powered flashlight is used as the light source. Two zip-ties secure the flashlight to a 3-axis adjustable stand, which is mounted to the frame of the schlieren system. The flash light is held in place and rotation is prevented by wedging blocks of rubber in between a square pattern of bolts that are tapped into the top surface of the stand and the flashlight. It is a pretty basic setup and could be made a little more professionally but the sub-assembly is secure and the light bulb provides enough light for the schlieren system to operate properly.[15]

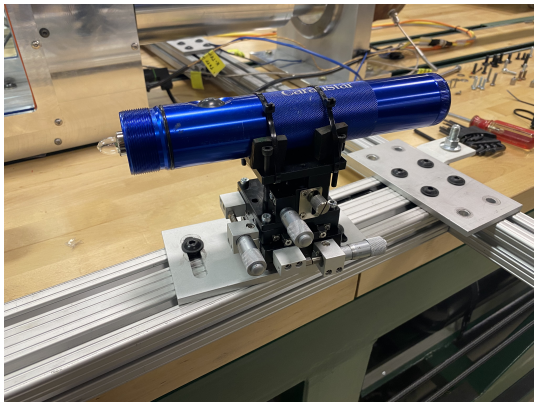

Figure 2.6: Light Source Assembly

2.2.1.3 Source Plane

The filters used by the schlieren system are of great concern to the operation of the system itself and the results provided by it. The Z-type schlieren system can produce black and white images as well as colored images depending on what filter is used. The production of black and white images requires that the light source is reduced to a point source. To do this the light is covered in all directions excluding one, very small hole on the face of the cover that points towards the schlieren mirror. The smaller the point source is, the higher the resolution of the schlieren image. To produce colored images, different colored and oriented filters are used to produce different types of results. The 2-Color Filter produces an image exactly like the black and white image but instead of black and white the colors of the filter are seen in the image. The ring lattice filter produces images that show the absolute magnitudes of refraction in light very well without giving any information about the direction of refraction. Lastly, the sector filter produces arguably the most beautiful color images of all, utilizing four different colors in its filter. This image, however, only displays the direction of the refraction of light and not the magnitude. [29]

2.2.1.4 Mirrors

The exit area of the nozzles used by the UNCC hypersonic wind tunnel is 4 inches so, a schlieren mirror with a diameter of 4 inches is used in the Schlieren system. A 15 degree Off-Axis parabolic Mirror was purchased off Edmund Optics instead of a regular parabolic mirror, to make the Z-type Schlieren system more effective. The critical dimension of the mirror is the focal length of 516.18 mm, which is exactly how far the light source and high-speed camera must be from their respective mirrors. The bolt patter on the back of the mirrors is required to properly secure the mirrors to the frame.

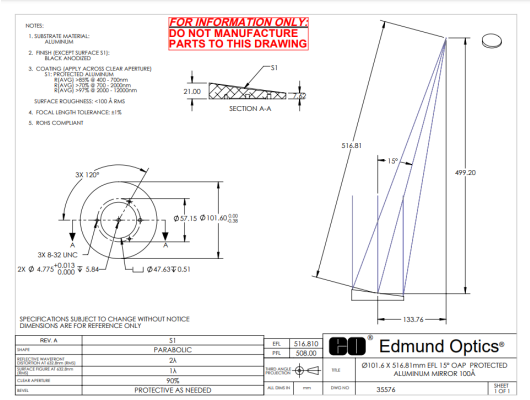

Figure 2.7: Drawing of parabolic mirror from Edmund Optics [23]

2.2.1.5 Mirror Assembly

When designing the method of securing the mirror to the Schlieren Frame plenty of constraints were considered. The mirrors need to sit at a very specific height above the top surface of the wind tunnel to see through the center of the viewing window of the test chamber. In order to achieve ease of alignment, the mirror must be secured to the frame in a way that it can be moved and rotated in all three dimensions at very small increments. Lastly, the mirrors themselves are very sensitive. So sensitive that just a fingerprint in the wrong area could require that the mirror is sent off to

be repaired. So, methods of protecting the mirror during inactivity, assembly and disassembly are required.

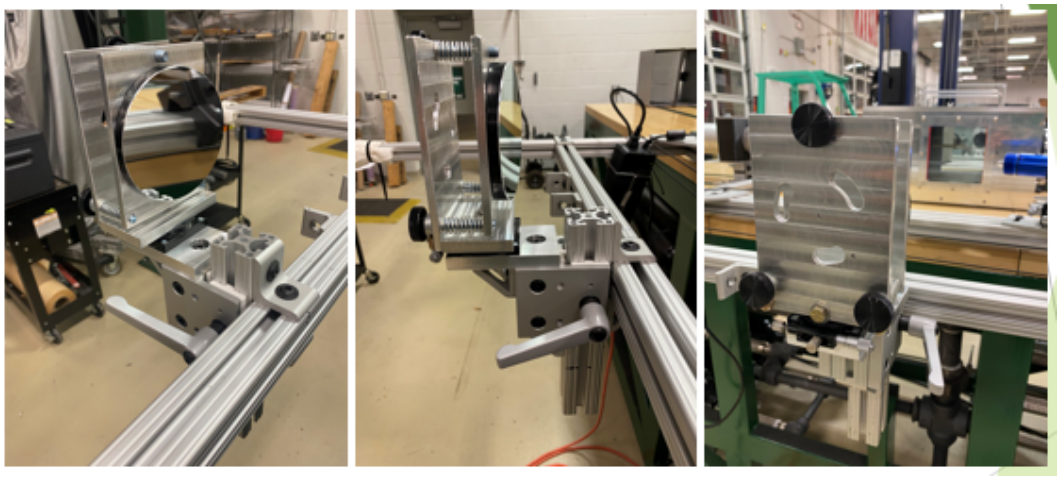

Figure 2.8: Mirror Assembly

As shown above in figure 2.8 the mirror is secured to a plate with a slotted pattern matching the bolt patter on the back of the mirrors. The plate is attached to another plate directly behind it by three bolts with springs in between the plates. This allows the mirror to be angled up and down easily by rotating the top bolt. The two plates holding the mirror in vertical position are mounted to a stage that allows fine-tune movement in all three axes as well as fine-tune rotation about the y-axis of the system. The stage is then mounted to a locking slide mount that is designed to fit on the 1.5 x 1.5 inch Aluminum extrusion used for the frame. This locking slide mount allows for the entire mirror assembly to be removed from the Schlieren frame quickly and easily when the schlieren system is inactive or being disassembled to change nozzles. When removed from the frame, the mirror assemblies are stored in a Pelican Case which is filled with foam that has cavities that fit the assemblies in a snug and secure manner. The last part of the mirror assembly fulfills another caution consideration. A cover, is 3-D printed out of a PLA polymer fits around the schlieren mirror for when the Schlieren system is inactive. The cover is held in place by the top bolt on the front

plate of the assembly and secured by a rubber band around both vertical plates of the assembly.

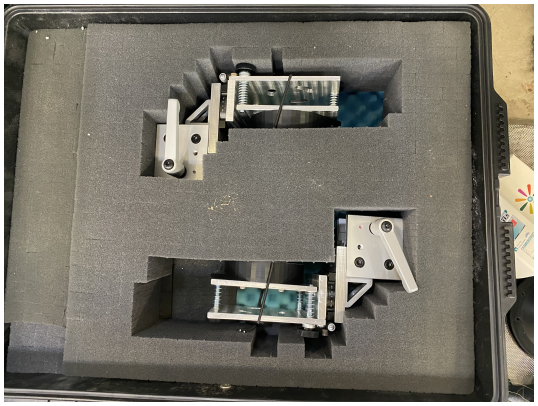

Figure 2.9: Mirrors, with protective cover, in Pelican case

2.2.1.6 Cut-off Plane

A very important component of the schlieren system is the cut-off plane. For monochromatic images the cut-off plane exists as a knife edge that blocks half of the light-path traveling from the second parabolic mirror to the camera. By doing this, some of the refracted light that is traveling through the medium (i.e. test chamber) is amplified in the final image, while some refracted light is blocked off by the knife edge.

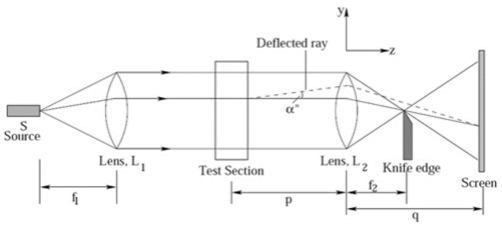

Figure 2.10: Visualization of how knife edge improves sensitivity to refracted light rays through test section

Figure 2.10 displays a simple schematic of how the knife edge increases sensitivity of the system to refracted light through a specific medium. The figure shows the

path of a light ray that is deflected by traveling from one medium to another (i.e. refraction) and how, after being deflected in the test chamber, the light ray responds to the lens it travels through. It is clear in Figure 2.10 that the light ray with a deflection angle of α makes it to the screen/camera. However, it should be equally clear that a light ray with a deflection angle of $-\alpha$ would be blocked by the knife edge from reaching the screen/camera. [22]

In order to understand this component and its purpose completely it is important to note that even though the knife edge blocks half of the path-ways of light between the second parabolic mirror and the camera, it does not entirely block any part of the resulting image when aligned properly. It is very important that the cut-off plane is placed exactly one focal length of the mirrors/lenses away from the second mirror/lens. If the knife edge is placed too close to the mirror, the knife edge will block part of the resulting image in the direction that it is coming from with respect to the mirror. If the knife edge is too far from the mirror, the knife edge will block part of the resulting image in the opposite direction that it is coming from. However, if the knife edge is placed at a perfect distance from the mirror, the knife edge will not block any part of the resulting image. Instead, the knife edge will only dim the brightness of the entire resulting image. Figure 2.11 displays this phenomenon where the knife edge is blocking light paths below the horizontal center line of the camera.

Figure 2.12 shows how the knife edge is supported and secured to the schlieren frame. The figure only shows how the monochromatic knife edge is secured in place. However, any type of cut-off plane required for color schlieren imaging can be created and secured to this mounting system with ease.

2.2.1.7 High Speed Camera

A MotionXtra HG-XR high-speed camera with a Nikon 80-200mm lens is used to collect images in this Schlieren System. The camera is capable of taking 100,000

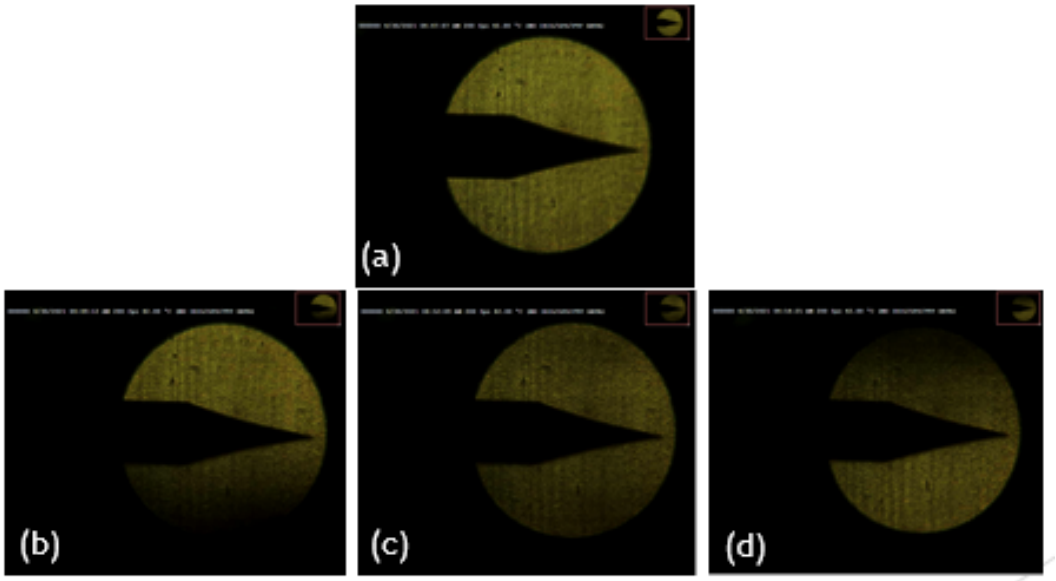

Figure 2.11: Visualization of results of a misplaced and perfectly placed knife edge. Resulting images of flared cone with (a) no knife edge in place; (b) knife edge too close to mirror, (c) knife edge in perfect position and (d) knife edge too far from mirror.

images per second at a very reduced resolution and 10,000 images per second with reasonable resolution. The camera is connected to a Dell computer with an Ethernet cable and run through a program called Motion Studio. In this program the critical settings of the camera can be adjusted such as the exposure and frame rate. Also, a live view of the line of sight of the camera can be seen on the monitor which is utilized during alignment of the entire system.

The camera is mounted to the frame of the Schlieren system in a very minimalistic way. Two L-brackets are secured to the mounting plate attached to the camera with 1/4 inch- 20 bolts and then the camera is secured to the frame with 5/8 inch-18 bolts. This method of assembly allows the camera to be freely and easily moved around in the X and Z axes of the system improving ease of alignment. This method does make movement in the Y axis impossible but as long as every other component is capable of moving up and down, they can all be aligned to the height of the camera lens making

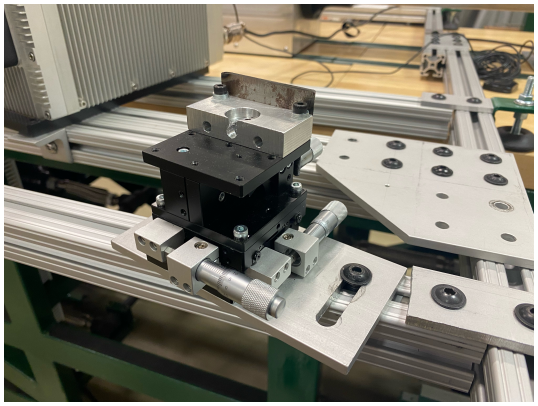

Figure 2.12: Knife Edge Assembly

Figure 2.13: Camera with Nikon Lens

that limitation unimportant.

2.2.2 Results

The results of the schlieren system lie solely in the quality of the resulting images. With that being said, the results provide quality, qualitative data about the airflow through the test chamber. This allows the schlieren system to be used as an educational tool, with the purpose of teaching students about optical measurement techniques and how to use them. Also, the qualitative data produced by this system will allow researchers to validate computational results under any conditions that the hypersonic wind tunnel is able to reach. Figure 2.14 displays two schlieren images of the air through the empty test chamber at Mach 5. The images are taken under identical testing conditions, the only difference between the two is that the image

labeled (b) is taken with the schlieren system shifted about 1.25 inches towards the front of the test chamber, relative to the position it was in while taking the image labeled (a). This figure displays distinct shock waves coming from the Mach 5 nozzle and the point at which the Mach waves bounce off of each other.

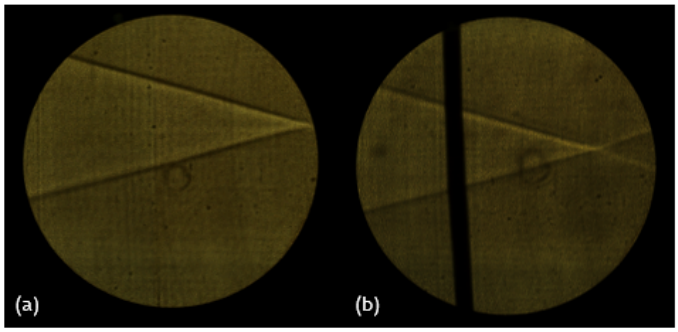

Figure 2.14: Schlieren images of air traveling through test chamber with no model in place

As a part of the initial testing, a simple cone model was created that could fit onto the stinger that was modeled by the senior design team. The cone was about 5/8 inches in diameter with a nose that came to a tip at a 17 degree angle to its base. The cone itself and the resulting monochromatic schlieren images taken of the cone at Mach 3 and Mach 5 are displayed in Figure 2.15.

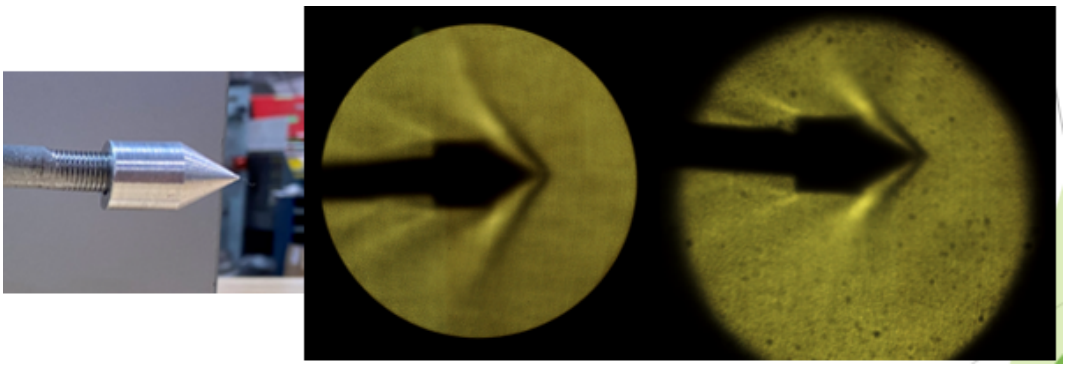

Figure 2.15: L->R: Image of cone model; schlieren image of cone model under Mach 3 and schlieren image of cone model under Mach 5

Later in the research process, a flared cone was designed and later fabricated to more accurately reflect hypersonic models. This cone was 1.5 inches long and de-

creased from a maximum diameter of 0.5 inches down to as much of a point as possible. The cone itself and the resulting schlieren image of the cone taken under Mach 5 flow are provided in Figure 2.16. It is important to note that the schlieren images of the flared cones were probably of the highest quality produced by this system. With that being said, the images would be drastically improved by making the same flared cone out of steel instead of aluminum. The high forces felt by the model while under Mach 5 flow caused the weakest point of the flared cone, the tip, to vibrate heavily during wind tunnel operation. This caused the fuzzy imaging at the tip that is seen in Figure 2.16and would be eliminated by having a model with a higher elastic modulus.

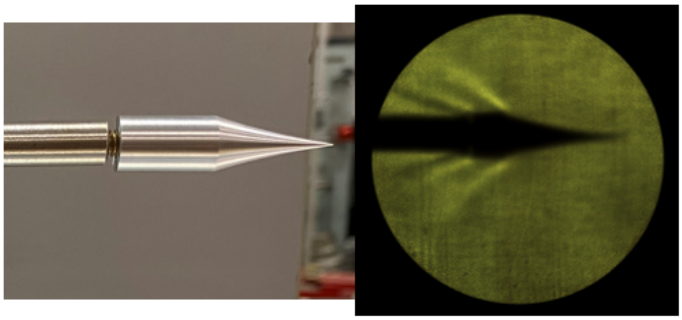

Figure 2.16: Schlieren image of flared cone model at Mach 5

CHAPTER 3: Linearly Actuated Pitot Tube System

The goal of this system is to measure the pressure of the air flow through the center of the test chamber. There are plenty of ways to achieve this. The simplest way would be to have a stationary system that reads the pressure during a test run and is adjusted in between each run to get new data at each point across the diameter of the air flow. This method would make it easy to support the pitot tube, as it would be secured to the top of the test chamber with a bulky stinger apparatus. However, this method would be extremely time consuming. Another method, would be to support the pitot tube in a way that allows it to be swept across the width of the test chamber while the wind tunnel is running. This method provides challenges in how the pitot tube will be supported without getting in the way of the flow of air, but if done properly, will provide a continuous set of data that can provide the user with a lot of information about how the wind tunnel is operating. The linearly actuated pitot tube design attempts to achieve the second method in order to add a sophisticated pressure sensing system to the UNC Charlotte hypersonic wind tunnel.

3.1 Theory

Research of the field of hypersonic research regarding supersonic and hypersonic wind tunnels suggests wide use of pressure transducers as the primary pressure sensing tool. A large portion of the explanation below regarding how pressure transmitters work is derived from "Hypersonic Wind Tunnel Techniques" which is reference [20] in the bibliography section.

3.1.1 Pressure Transducer

A pressure transducer, like all sensors, is a system that converts a mechanical response to its environment to an electrical signal. Inside the sensor there are two cavities separated by a flexible diaphragm. One of the cavities holds a known amount of pressure and is considered to be the reference side. The second cavity has an opening that is connected to the measured environment. A strain gauge is integrated with the diaphragm that produces a signal according to how much the diaphragm flexes. So, if the measurement side holds a pressure that is much less than that of the reference side, the diaphragm will deflect towards the measurement side and the strain gauge will produce a negative signal that varies in strength depending on how much lower the measurement pressure is than the reference pressure. Similarly, if the measurement side holds a pressure greater than the reference pressure, then the diaphragm will deflect towards the reference side and the strain gauge will produce a positive signal relative to the difference in pressures between the measurement side and reference side. A schematic of a pressure was extracted from reference [20] and provided below for a clearer understanding.

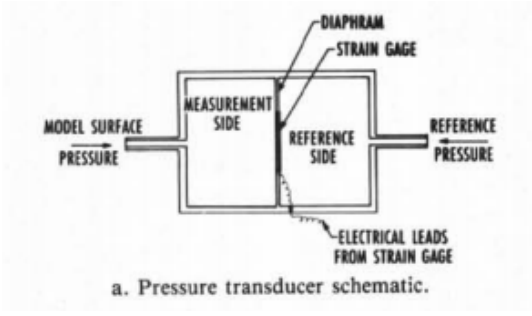

Figure 3.1: Schematic of Pressure Transducer

3.1.2 Pitot Tube

The staple tool used to provide a pressure reading to a pressure transducer is a pitot tube. The pitot tube is a very simple device that exposes the cavities of the pressure transducer to the measurement environment. The tip of the pitot tube is

piece of metal that varies in thickness and has multiple paths for air to travel through inside of it. One of the air paths is directly through the center of the pitot tube and this air path measures the total air pressure of the air flow the pitot tube is subjected to. The rest of the air paths surround the total pressure air path and exit the pitot tube radially to measure the static pressure of the air flow that the pitot tube is subjected to. An image of a labeled diagram of a pitot tube is provided in Figure 3.2 below for a clearer understanding. [4]

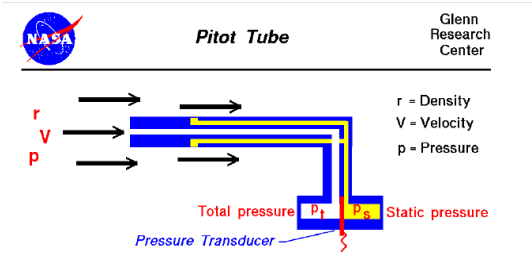

Figure 3.2: Pitot Tube Schematic

A total pressure and static pressure reading of the flow field allows the user to use Bernoulli's equation to calculate dynamic pressure. Then, when relevant, Bernoulli's equation can be manipulated to calculate the free stream velocity of the environment. Bernoulli's equation and its manipulation are displayed below in equations (3.1) and (3.2).

$$P_s + P_d = P_t \tag{3.1}$$

where:

P_s = static pressure

P_d = dynamic pressure

P_t = total pressure

$$P_d = \frac{r * V^2}{2} \tag{3.2}$$

where:

P_d = dynamic pressure

r = density

V = velocity

3.1.3 Linear Actuator

A linear actuator is a mechanism that utilizes a DC motor to rotate a lead-screw by connecting the two with a set of gears. The arm of the linear actuator is connected to a slider that is tapped on the lead-screw the same way a bolt would be and restricted from rotating but allowed to move along the length of the lead screw. The slider and arm move away from the base of the lead screw or towards the base of the lead-screw depending on direction of rotation of the lead-screw. Since the direction of rotation of the lead-screw is dependant on the direction of rotation of the DC motor, it understood that the direction of travel of the arm of the linear actuator is dependant on the direction of current flowing through the motor. [7]

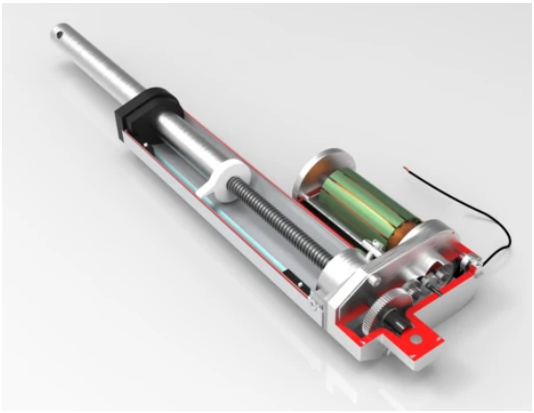

Figure 3.3: Linear Actuator Schematic

Linear actuators are differentiated in a few ways. The most crucial being in the speed at which the arm retracts and extends, as well as the load it can push and pull. These discrepancies are identified in the specs of the gear ratio and the motor size

and are almost always identified in the part specs provided by the supplier.

Another difference that exists among linear actuators is the inclusion of limit switches or feedback in the mechanism. Some linear actuators have limit switches built into the frame that engage and disengage as the arm moves to full extension or retraction. The limit switches are crucial to not ruining the system because if the lead-screw drives the slider too farm in towards the gears of the actuator or too far out of the frame, the whole mechanism can ruin itself without enough attention. If there are no limit switches, there is typically a feedback system that utilizes a potentiometer to read the distance of the arm with respect to its fully retracted position. The potentiometer works with two parts. First is a resistor or set of resistors that exist along the length of the lead-screw. The second is a node, most likely attached to the slider, that allows current from the string of resistors to pass. The same power supply that powers the motors travels through the string of resistors and can be read by a voltmeter. Another voltmeter reads the voltage across the string of resistors only up until the node is making contact. The difference between the voltmeter readings of the supply voltage and the node voltage correspond with a specific location of the slider and arm along the length of the lead-screw. It is important to note that while a potentiometer can identify the location of the arm of the slider, it is almost never programmed to stop the actuator from over or under traveling. So, a set of external limit switches are required to maintain the actuator's integrity.

3.1.4 Rayleigh Pitot Tube Formula

In order to calculate the Mach number of the air traveling through the test chamber, the Rayleigh Pitot Tube Formula will be used. The equations is a slight manipulation of the pressure ratio formula referenced in the De Laval nozzle section of this paper. Put simply, the equation equals the ratio between the total pressure reading from the pitot tube (P_{02}) and the stagnation pressure before the bow shock at the tip of the pitot tube (P_1). [19] Equation (3.3) allows researchers to calculate the mach number

of the air flow measured by the pitot tube.

$$\frac{P_{02}}{P_1} = (\frac{(\gamma+1)^2(M_1)^2}{4\gamma(M_1)^2 - 2(\gamma-1)})^{(}\frac{\gamma}{(\gamma-1)}\frac{1-\gamma+2\gamma(M_1)^2}{\gamma+1} \tag{3.3}$$

3.2 Design

The UNC Charlotte wind tunnel relies on the test chamber acting as a vacuum to reach its mach numbers, so the pitot tube, first a foremost, needed to be integrated into the test chamber in a way that would not expose the test chamber to the outside environment. To do this, the Pitot Tube Fitting sub assembly was designed to fit around the pitot tube, creating an air tight seal in the test chamber while still allowing the pitot tube to move freely through the center of the sub assembly. This sub assembly consists of various washers and spacers encased in a plastic compression tube fitting with a male 3/4" NPT thread. The pitot tube fits through this sub assembly and the compression tube fitting is secured to a female 3/4" NPT thread tapped into the sidewall of the test chamber.

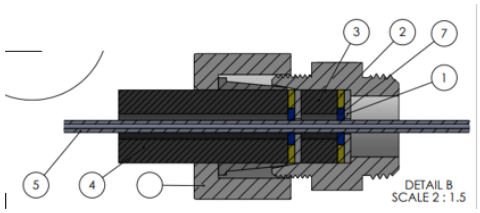

Figure 3.4: Pitot Tube fitting sub-assembly

In order to sweep the pitot tube across the width of the test chamber, a motor needed to be incorporated that could be secured to the pitot tube while pushing and pulling it back and forth in the test chamber. An Actuonix P16 linear actuator was chosen. A small but low tolerance mount was required to integrate the linear actuator with the the pitot tube. the pitot tube needs to be pushed very accurately in one direction back and forth with minimal 'wobble' so the mounting system leaves

very little room for error. The pitot tube support sub assembly displayed below in Figure (3.5) was designed specifically for this system and machined on a mill at UNC Charlotte.

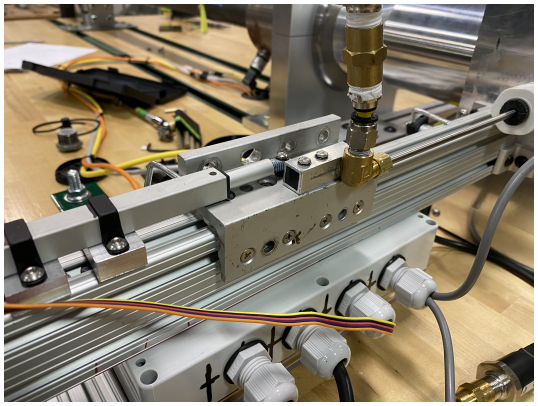

Figure 3.5: Pitot tube-to-actuator mounting system

It is important to note that linear actuators are subject to being over driven in one direction or another. So, limit switches are required to be used with a linear actuator to prevent over-driving and ruining the linear actuators. This requires another consideration which is the support of the entire system. Instead of standing on its own, the system is designed to be mounted to the side of the test chamber on an 1"x2"x19" piece of aluminum extrusion with three L brackets. The linear actuator is secured to the top face of the aluminum extrusion with special made mounts at a very specific height. The limit switches are secured to the side face (either side) of the aluminum extrusion at specific distances along the length of the extrusion according to the placement and capabilities of the linear actuator.

A simple back of the napkin calculation will show that a 1/8" pitot tube will not survive the forces it would feel from the air traveling through the center of the test chamber. So, the final consideration is concerning how to support the pitot tube as it travels across the width of the test chamber without impeding its motion or the airflow. To achieve this the pitot tube support assembly was designed which features a 1/8" thick piece of steel with a 1/8" semicircular groove machined into it that serves

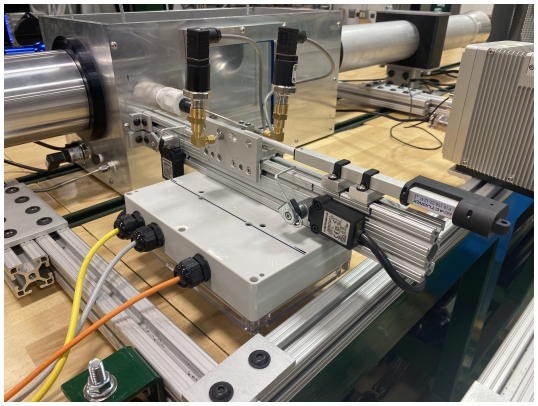

Figure 3.6: Linearly actuated pitot tube assembly mounted to sidewall

as the primary support piece. Two mounts with slots in them allow the horizontal support piece to be secured to both sidewalls with 1/4"-20 bolts. The assembly is designed with slots instead of clearance/threaded holes to provide the system with freedom in all axes, allowing the support system to be leveled and perfectly coincident with the pitot tube. Concerns with the pitot tube jumping out of its slot on the horizontal support piece led to the addition of two pieces of sheet meal on the top and bottom surface of the support piece. The sheet metal is high strength stainless steel and was welded to the horizontal support piece.

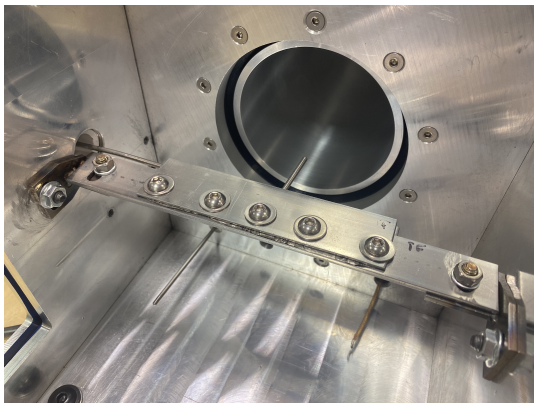

Figure 3.7: Pitot tube support sub-assembly

3.2.1 Circuit Design and Control Considerations

The UNC Charlotte wind tunnel was completed well before the linearly actuated pitot tube system was designed so the linear actuator could be controlled with the

wind tunnel's existing control system. The detailed circuit diagram is provided in Appendix B at the end of this document. All moving parts of the wind tunnel are controlled by a PLC programmed with DirectSoft, a program provided by Automation Direct. All of the sensors provide their signals to LabView which reads the signals and displays them on the display window. It made sense to control the movement of the linear actuator with the PLC powered by three different push buttons. The direction of travel of the linear actuator is dependent on the direction of the current through the motor. So, it is wired up to the PLC through two relays. The position of the first relay determines whether or not the motor recieves power from the PLC while the position of the second relay determines the direction of the current flowing through the motor. The program in DirectSoft controls the three push buttons accordingly. The first push button labeled 'Extend' commands the linear actuator to extend its arm until the over travel limit switch engages, which tells the system to turn off power supply to the actuator. The second button labeled 'Retract' commands the linear actuator to retract it's arm until the under travel limit switch engages. The third push button labeled 'Sweep' commands the linear actuator to extend its arm until the over travel limit switch engages, which commands the actuator to retract the arm until the under travel limit switch engages, which commands the actuator to extend its arm. The program cycles through the extension and retraction of the arm until the push button is released by the user.

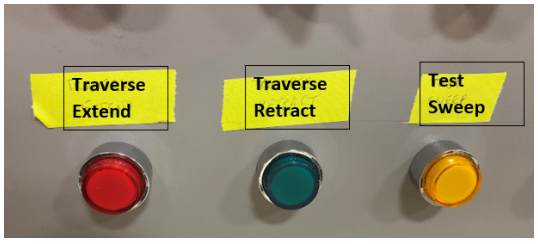

Figure 3.8: The three buttons that control the linear actuator's extend, retract and sweeping capabilities

The sensing mechanisms of the linearly actuated pressure sensing system all provide signals to the LabView program that receives signals from all of the sensors throughout the wind tunnel. The pressure transducers that measure total and static pressure are wired to analog input slots of the SCXI module below the control box of the wind tunnel. Parallel to that, the position of the arm of the linear actuator is read by measuring the voltage across the potentiometer built into the linear actuator. This is done by wiring the power supply to an analog input of the SCXI and wiring the potentiometer node to another analog input. The difference between the two voltage readings corresponds to the position of the arm of the linear actuator. If the voltage readings are equal, the arm is retracted all the way back into the linear actuator, and if the difference between voltage readings is at a maximum, the arm is fully extended.

3.3 Results

the linearly actuated pitot tube system was designed to provide users with information about the air flow through the center of the test chamber. The pressure data can tell the user what the speed of the air passing through the test chamber is. The sweeping capability of the system allows the user to identify the diameter of the stable region of the flow field. The continuous nature of the data collection allows the user to asses and quantify the stability of the flow over time at different locations across the width of the test chamber. However, support of the pitot tube proved to be much more difficult than expected. Initially, a pitot tube with a 1/8" diameter was used and the support system was minimal but ended up being far too weak to endure Mach 5 flow. The thin pitot tube and the minimal support system was designed intentionally to minimize frontal area of the measurement system. Since the initial design was too flimsy to endure Mach 5, a much more secure system was designed that still considered frontal area but with much less importance than the original design. With that being said, the stronger system proved to be much more secure. The pitot tube could traverse back and forth across the width of the test chamber

as well as take data. The data was then extracted from the LabView program and the Mach number value was calculated using Equation (3.3) and plotted against the position of the pitot tube, which is provided in Figure 3.9.

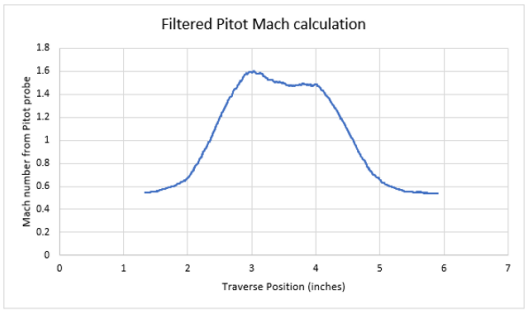

Figure 3.9: Rayleigh Pitot mach calculation plotted against traverse position extending

The graph in Figure 3.9 shows the maximum Mach number achieved in the wind tunnel is only 1.6, when it should have been Mach 5. This is definitely because the frontal area of the pressure measurement system is far greater than the allowed 10 percent.

CHAPTER 4: Manifold Addition

In order to produce air flow that travels at hypersonic speeds (Mach 5 and 7), the manifold of the hypersonic wind tunnel has been designed to hold up to 2400 PSI. However, due to some leakage the maximum PSI reaches has been about 1500 PSI, which is still sufficient to reach hypersonic speeds. In the same lab as the hypersonic wind tunnel there exists a rocket nozzle test table. This table provides a rocket nozzle and its exiting air flow to be visualized clearly with a schlieren system. The rocket nozzle testing table has produces beautiful visualization of air flow patters exiting a rocket nozzle with monochromatic and color schlieren imaging. The rocket nozzle test stand at UNC Charlotte requires only about 100 PSI to serve its purpose. However, a higher volume and pressurized air source would expand the capabilities of the rocket nozzle test stand.

Figure 4.1: Rocket Nozzle test stand in the Motorsports Research building at UNC Charlotte

So, a change in the manifold of the hypersonic wind tunnel was designed and implemented in order to more easily provide the high pressure and high volume air supply held in the manifold of the hypersonic wind tunnel to the rocket nozzle test stand

without interrupting the function of the wind tunnel. This was done by replacing the vertical pipe on the back end of the wind tunnel, that existed directly before the electronically actuated fast valve, with a tee fitting and a pipe plug.

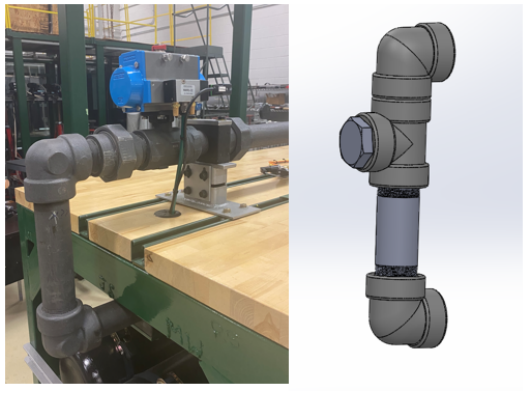

Figure 4.2: Old manifold (left) and Manifold addition design (right)

Obviously, the pipe plug is tapped into the tee fitting while the manifold supplies air to the hypersonic wind tunnel nozzle. In order to supply air to the rocket nozzle test stand the pipe plug must be removed and a series of fittings that are designed to reduce the pipe diameter down to fit the tube used to supply air to the rocket nozzle as well as provide easy assembly and disassembly of the integrated system. Once the pipe plug is removed, a 2" NPT male to 1: NPT female adapter is tapped into the tee fitting fitting with a 1" NPT nipple fitting connecting the adapter to the front end of a 1" NPT union. The other end of the union is connected to a manually actuated ball valve rated to hold 3000 PSI with another 1" NPT nipple fitting. The other end of the ball valve has the previously used flexible tube tapped into it, which is also rated to hold 3000 PSI. In order to improve the ease of use and practicality of the system, a 1" female NPT to 1" female NPT connector is used to connect two flexible hoses which doubles the available length between the hypersonic wind tunnel manifold and rocket nozzle connecting port.

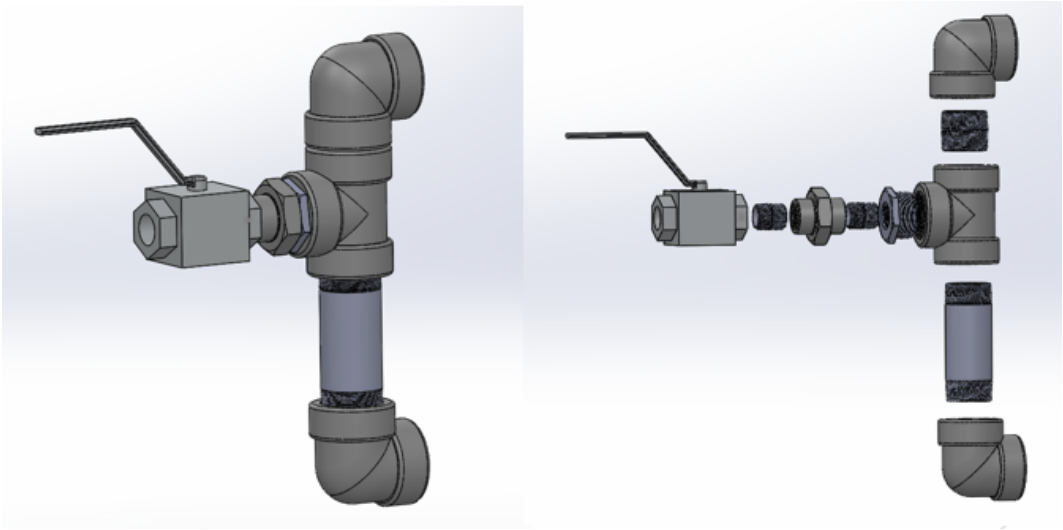

Figure 4.3: Manifold addition assembled to supply air to the rocket nozzle test stand on the left. Blown up assembly of the manifold addition on the right

CHAPTER 5: Stinger Re-Design

The stinger, designed to hold test models and instrumentation in the test chamber, was re-designed to better serve its purpose. Decreased frontal area and a more optimal model mounting method are the two primary improvements. In order to identify how the two improvements were made, the differences between the design of the old and new stingers must be addressed.

Figure 5.1: Old Stinger Design

The old stinger features two components; a T-shaped body and a shaft. The stinger consists of two 1/8" thick plates of mild steel welded together. The top of the "T" has a four hole pattern that matches the threaded hole pattern on the lid of the test chamber. Each hole has more than enough clearance for 1/4"-20 bolts. The vertical plate of the stinger has two rounded slots that travel the along the length of the plate. The rounded nature of the slots allow for the shaft to be angled up and down while maintaining the position of the model with respect to the flow of the air through the test chamber. The slots extend all the way down to the bottom face of the plate in a way that allows the shaft to be secured to the plate parallel to the flow of the air.

The length of the shaft is 8", which is the required length to have the model extend to the middle of the viewing windows of the test chamber. The back end of the shaft has a square cross section with a little over a 1/8" wide straight slot down the length of it. The straight slot is just wide enough to fit around the vertical plate of the body of the stinger. Two clearance holes in the back end of the shaft allow two bolts to fit through the shaft as well as the rounded slots on the vertical portion of the body of the stinger and clamp the shaft to the body. The front end of the shaft has a circular cross section of 3/8" diameter that was created by putting the square stock in a lathe. The outer surface of the tip of the shaft is threaded so that models with a 5/16"-18 tapped hole can be secured to it.

5.1 New Stinger

Figure 5.2: New Stinger Design

The new stinger features two bodies of similar mass made out of 1/4" mild steel plates. The first body is very reminiscent of the body of the old stinger. The top of the T-shaped body has a hole pattern identical to that of its predecessor and the vertical portion of the body has two rounded slots that run down the length of the plate. The only difference is that the slots and plate of this body are reduced (compared to the old stinger body) from 4.25" to 1.5". The second body of the new stinger is a 4"x3" plate with a 3/8" shaft butt welded along the edge of the plate that is 4" long. At the top of the second stinger body, there are two 1/4"-20 tapped holes that allow for

the second body to be secured to the first body as long as the bolts are sent through the slots of the first body. The length of the shaft of the second body extends 7". It is worth mentioning that the length of the new shaft is about an inch shorter than the length of the old shaft. This is because instead of threading the outer surface of the tip of the shaft, a hole was drilled into the shaft and an M6 thread was tapped into the end of the shaft. Doing the drilling and tapping of the tip of the shaft on a lathe ensures that the tap is straight with a tolerance of plus or minus a fraction of a degree which ensures that alignment of the model tapped into the shaft is as easy as possible.

5.2 Notable Improvements

The differences between the two stingers provide two notable improvements of the newly designed stinger. The first is a reduced frontal area of the stinger. By changing the way that the shaft is mounted to the stinger, the bolts required to clamp the stinger together are removed from the air flow region. So, the frontal area of the stinger is reduced from 0.923 in^2 to 0.563 in^2 which is a 40 percent reduction.

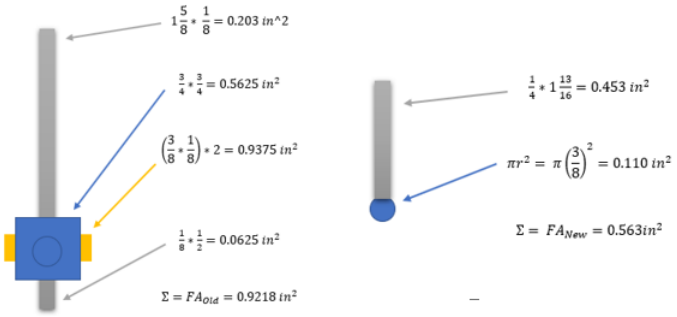

Figure 5.3: Frontal area calculations of old stinger (left) and new stinger(right)

The second notable improvement is the method by which the test models are mounted to the stinger. To be fair, a very high quality of component manufacturing would negate this improvement. The improvement can really be credited to the ease in manufacturing. The ability to make an almost perfectly straight tap on a lathe is

much higher than the ability to make an almost perfectly straight thread on a shaft with a die in a vice. With that being said, the tap in the new stinger is straight to a much higher tolerance than the original stinger, which improves ease of alignment of the model significantly.

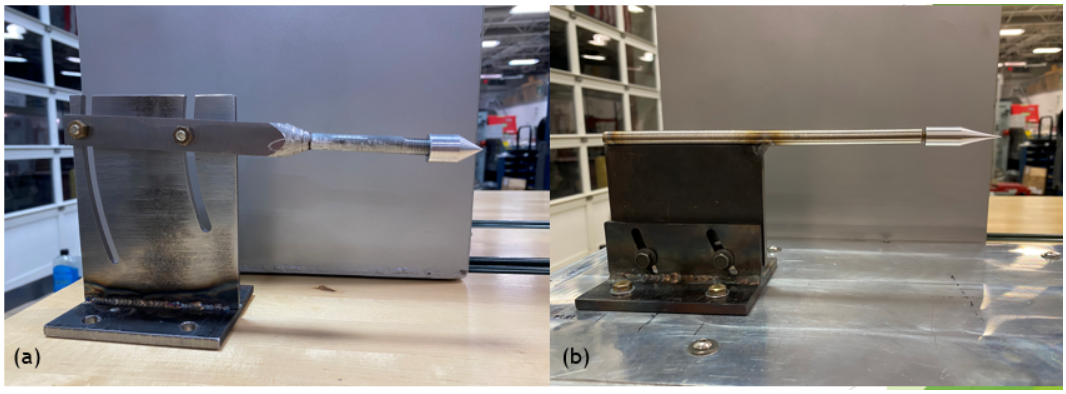

Figure 5.4: Visualization of the (a) old stinger with cone model assembled and (b) new stinger with flared cone model assembled

In addition to how the model is mounted to the end of the stinger, a leveling system has been created to ensure that the stinger shaft is parallel to the lid of the test chamber. This is used with the leveling piece that is designed to sit on outer surface of the shaft and be secured with an M6 bolt that threads into the tip of the shaft. The stinger is bolted to the lid of the test chamber, with the lid rests upside down and flat on the top surface of the wind tunnel. Then, with the leveling piece secured to the tip of the stinger, the orientation of the second body with respect to the first body of the stinger can be adjusted and locked in place with the bolts that fit through the slots on the first body. Figure (5.5) below provides a visualization of how the leveling piece is incorporated with the stinger.

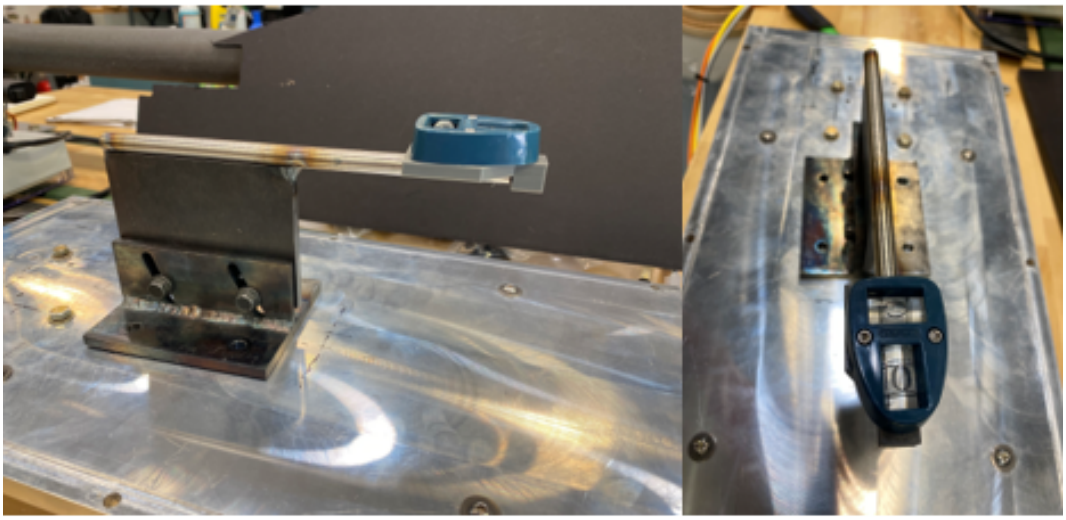

Figure 5.5: Stinger leveling system

CHAPTER 6: Future Experiments

6.1 Past Experiments

6.1.1 Aerodynamic Heating over Flared Cones

The three challenges in advancement of hypersonic flight and the vehicles used to achieve it are the high heat transfer rate from the air around the vehicle to the vehicle, material selection regarding what the hypersonic vehicle will endure and aerodynamics of the vehicle. One particularly interesting study titled *"Hypersonic aerodynamic heating over a flared cone with wavy wall"* [30] was completed in April 2019 at Peking University. In this study a flared cone with and without a waved surface pattern was exposed to Mach 6 winds. the study used Rayleigh-scattering flow visualization and high-thermal-sensitive infrared thermography to study the stability of the air traveling along the surface of the flared cone. The study found that the flared cone with a smooth wall lost its flow stability a little after 90 percent of its length. The flow detached from the flared cone and went completely turbulent which correlates strongly to high enthalpy between the environment and the modeled vehicle. The flared cone with a wavy wall maintained its flow stability across the entire length of the flared cone while maintaining a sharper and smaller boundary layer on the back end of the flared cone, with respect to the flared cone with a smooth wall. The Rayleigh scattered flow visualization results of this experiment are provided below in Figure (6.1).

At the same time, the infrared data showed that the smooth walled flared cone had two hot spots during the experiment where the heat transfer between the air flow and the model is particularly high. The same data taken on the wavy walled

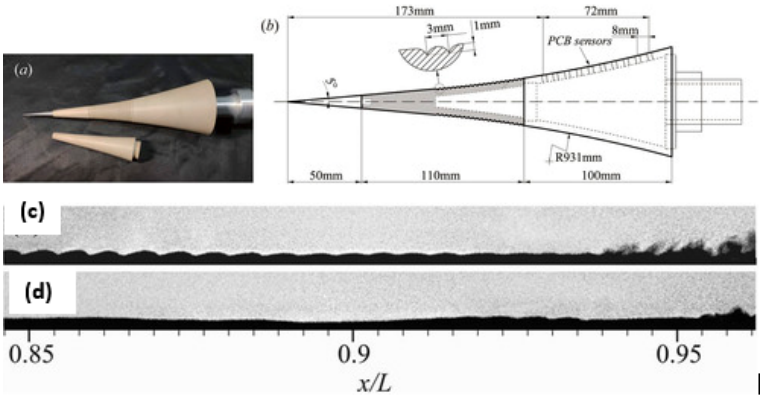

Figure 6.1: This figure displays the model (a) with and (b) without wavy walls as well as the Rayleigh-scattering flow visualization results for the (c) smooth cone and (d) flared cone

flared cone showed that both hot spots were completely eliminated. The elimination of the hot spots can be attributed, at least a little bit, to the improved flow stability found between the two models. The IR data from the experiment is displayed below in Figure (6.2)

6.1.2 Visualization of Shock Wave Phenomenon around a sharp Cone

Another interesting study from the MIT Department of Aerospace Engineering titled *"Visualization of Shock Wave Phenomenon around a Sharp Cone Model at Hypersonic Mach Number in a Shock Tunnel using High Speed Schlieren Facility"* studied the propagation of a shock wave over a sharp cone model exposed to air traveling at mach 6.5. The study used a highly compressed driver tube to send air through a shock tube towards a Delaval nozzle. Beyond the nozzle is a cavity that serves as the test section and dump tank, which is where the model is suspended at a zero degree angle of attack as well as a 5 degree angle of attack. The paper specifies the expected shock angles of a cone with an angle of 11.38 degrees to the base with calculated values. The paper also provided CFD results for both angles of attack as a reference. The shock angles viewed by the schlieren system validate their calculations as well as their CFD. A collection of the results is provided in Appendix C for a better

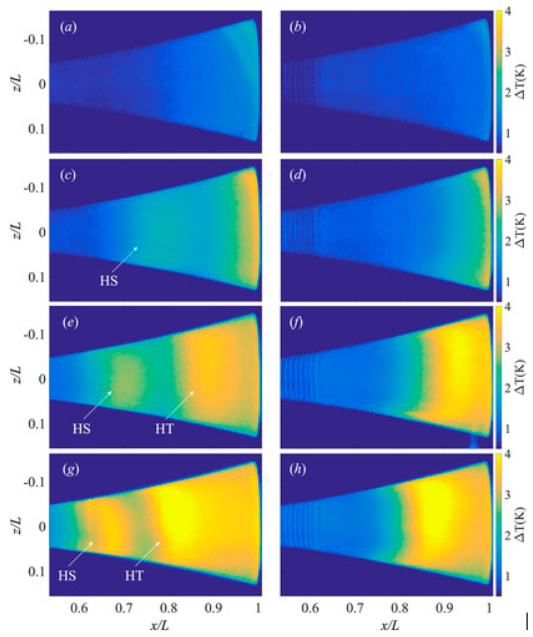

Figure 6.2: Thermal data for smooth and flared cones taken with high speed IR sensitive camera over time

understanding of the purpose and results provided by the paper. [27]

6.2 Future Experiments

The two experiments referenced in the section above are good starting points for research on the UNC Charlotte hypersonic wind tunnel. This is because, both experiments validate accepted understanding of how a wind tunnel and schlieren system should work with each other and the UNC Charlotte wind tunnel is capable of emulating the experiments. Comparable results would validate the each system individually along with their integration with each other.

The only difference worth mentioning is that the wind tunnels used in the experiments have a higher flow volume and therefore, larger models than the UNC Charlotte wind tunnel could hold. So, scaling down the models before imitating the experiments should be a part of the process.

REFERENCES

[1] Actuonix. *www.actuonix.com*, www.actuonix.com/P16-S-Linear-Actuator-p/p16-s.htm.

[2] Anderson, John D. Hypersonic and High-Temperature Gas Dynamics. *American Institute of Aeronautics and Astronautics*, Inc., 2019.

[3] Barlow, Jewel B., et al. *Low-Speed Wind Tunnel Testing*. Wiley, 1999.

[4] Benson, Tom. "Pitot Tube." *NASA*, www.grc.nasa.gov/www/K-12/VirtualAero/BottleRocket/airplane/pitot.html.

[5] Chang, Wilbur. "Design and Development of a Rectangular Supersonic Wind Tunnel Facility for the Study of Shock/Boundary Layer Interactions."

[6] Chu, Peter, et al. Aerospace Research Centeral, 2012, *High Temperature Storage Heater Technology for Hypersonic Wind Tunnels and Propulsion Test Facilities*.

[7] "Classic Rod Linear Actuators." *Firgelli Automations*, www.firgelliauto.com/products/linear-actuators.

[8] "Comatic Aberrations." *Optical Aberrations - Comatic Aberrations - Java Tutorial | Olympus LS*, www.olympus-lifescience.com/fr/microscope-resource/primer/java/aberrations/coma/.

[9] "Comparison of Optical Aberrations: Edmund Optics." *Edmund Optics Worldwide*, www.edmundoptics.com/knowledge-center/application-notes/optics/comparison-of-optical-aberrations/.

[10] Davidhazy, Andrew, "Introduction to shadowgraph and schlieren imaging" (2006). Accessed from http://scholarworks.rit.edu/article/478

[11] Dyke, Milton Van. *An Album of Fluid Motion*. The Parabolic Press, 2012.

[12] Eschenbach, R.C., and G.M. Skinner. n.d., *Development of Stable, High Power, High Pressure Arc Air Heaters for a Hypersonic Wind Tunnel*.

[13] Idris, Azam Che, et al. PubMed.gov, 2014, *Luminescent Measurement Systems for Investigation of Scramjet Inlet-Isolator*.

[14] "Introduction to Mirrors." *Basic properites of Mirrors - Introduction to Mirrors | Olympus LS*, www.olympus-lifescience.com/en/microscope-resource/primer/lightandcolor/mirrorsintro/.

[15] Kook, Sanghoon, et al. Society of Automotive Engineers of japan, 2011, *Z-Type Schlieren Setup and Its Application to High-Speed Imaging of Gasoline Sprays*.

[16] Libretexts. "Snell's Law." *Engineering LibreTexts*, 21 Oct. 2020, eng.libretexts.org/Bookshelves/Materials-Science/Supplemental-Modules-(Materials-Science)/Optical-Properties/Snell's-Law.

[17] "Limit Switch." *AutomationDirect*, www.automationdirect.com/adc/shopping/catalog/sensors-z-encoders/limit-switches/plastic-compact-limit-switches/side-rotary-adjustable-rod-actuator/aep2g71z11-1.

[18] Lockheed Martin Misiles and Fire Control. *High Speed Wind Tunnel and Test Systems Design Handbook.* Publication Number AER-EIR-13552-E, 5/06/2002

[19] Massachusetts Institute of Technology, 2008, *Fluids-Lecture 16 Notes.*

[20] Matthews, R.K., and R.W. Rhudy. Calspan Corporation/AEDC Operatios, 1993, *Hypersonic Wind Tunnel Test Techniques.*

[21] Mazumdar, Amrita. 2013, *Principles and Techniques of Schlieren Imaging Systems.*

[22] NPTEL, 2012, *Intorduction to Schlieren and Shadowgraph.*

[23] "Off-Axis parabolic Mirror." *Edmund Optics Worldwide*, www.edmundoptics.com/p/1016-x-508mm-pfl-15-off-axis-parabolic-aluminum-mirror/33448/.

[24] Oudheusden, Bas, and David Watt. 2004, *Assessment and Application of Quantitative Schlieren Methods: Calibrated Color Schlieren and Background Oriented Schlieren.*

[25] Pavlov, A., and M. Golubev. n.d., *Some Aspects of a Schlieren Technique Sensitivity Increasing.*

[26] Pope, Alan. *Wind Tunnel Calibration Techniques.* Sandia Corporation, Apr. 1961

[27] Saiprakash, M., and C. SethilKumar. Journal of Applied Fluid mechanics, 2019, *Visulaization of Shock Wave Phenomenon around a Sharp Cone Model at Hypersonic Mach Number in a Shock Tunnel using High Speed Schlieren Facility.*

[28] "Schlieren Optics." Harvard Natural Sciences Lecture Demonstrations. Harvard Natural Sciences Lecture Demonstrations, 2021, Cambridge, Science Center.

[29] Settles, G.S. 1981, *Color Schlieren Optics - A Review of Techniques and Applications.*

[30] Si, Wufei, et al. AIP, 2019, *Hypersonic Aerodynamic Heating over a Flared Cone with Wavy Wall*

[31] Solomon, Jason. âThe Design, Calibration, and Commissioning of a Benchmark Hypersonic Wind Tunnel.â *University of North Carolina at Charlotte*, 2021.

[32] Zheng, Ri Sheng, et al. âOptimal Classification of Hypersonic Inlet Start/Unstart Based on Manifold Learning.â *Applied Mechanics and Materials*, vol. 274, 2013, pp. 200â203., doi:10.4028/www.scientific.net/amm.274.200.

APPENDIX A: P16 Linear Actuator Data Sheet

P16 Specifications

Gearing Option	22:1	64:1	256:1
Peak Power Point	40N @26mm/s	80N @9mm/s	250N @2.5mm/s
Peak Efficiency Point	25N @34mm/s	40N @14mm/s	150N @3.4mm/s
Max Speed (no load)	46mm/s	18mm/s	4.8mm/s
Max Force Lifted	50N	90N	300N
Back Drive Force	75N	200N	>500N

Stroke Option	50mm	100mm	150mm	200mm
Mass	95g	110g	125g	140g
Repeatability (-P & LAC)	0.3mm	0.4mm	0.6mm	0.8mm
Max Side Load	20N	15N	10N	4N
Closed Length hole to hole	97mm	147mm	197mm	247mm
Feedback Potentiometer	6kΩ±50%	11kΩ±50%	20kΩ±50%	23kΩ±50%

Feedback Linearity	Less than 2.00%
Input Voltage	0-15 VDC. Rated at 12VDC.
Stall Current	1000mA @ 12V
Operating Temperature	-10°C to +50°C
Audible Noise	62 dB @ 45cm
Ingress Protection	IP-54
Mechanical Backlash	0.3mm
Limit Switches (-S)	Max. Current Leakage: 8uA
Maximum Static Force	500N
Maximum Duty Cycle	20%

APPENDIX B: Circuit Diagram for linearly Actuated Pitot Tube

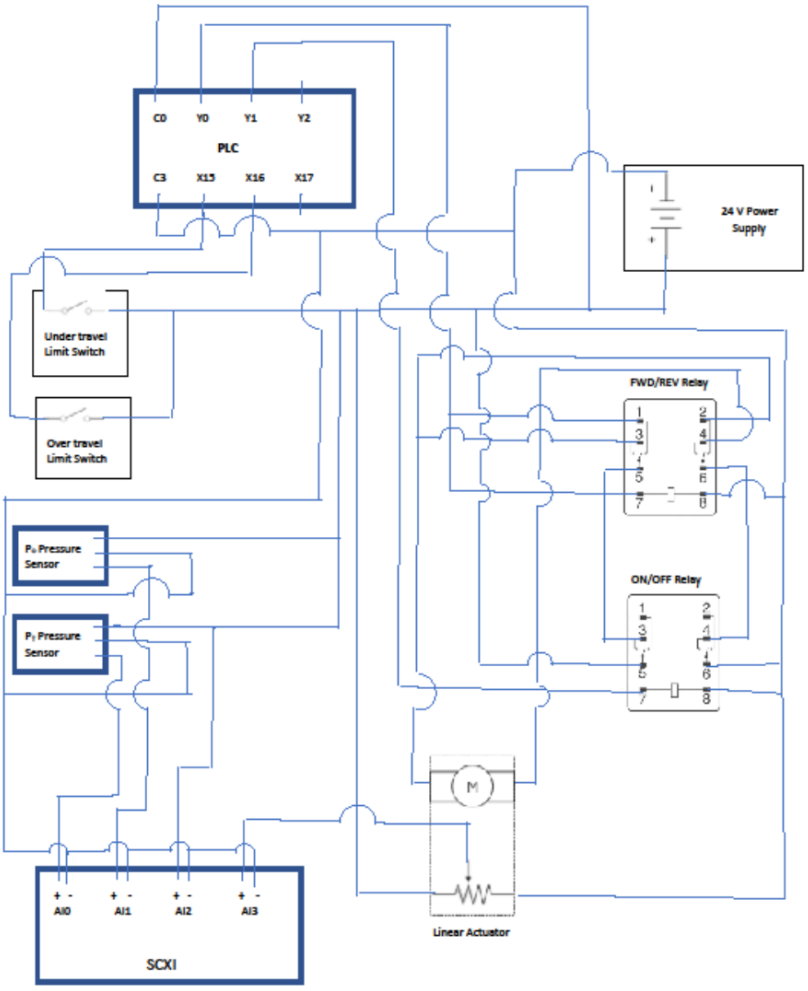

APPENDIX C: Results of Flow Visualization of Sharp Cone Experiment

	M=6.5	M = 6.5	
	α= 0°	α= 5°	α= 5°
		Windward direction	Leeward direction
Experiment	15.2°	20.1°	Not able to capture
Theory	15.1°	20.0°	10.9°
Computation	15.1°	20.2°	10.8°

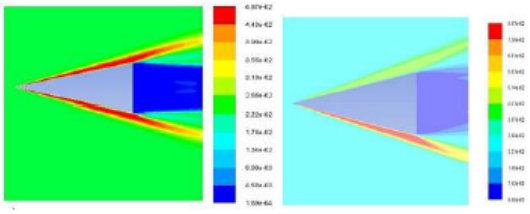

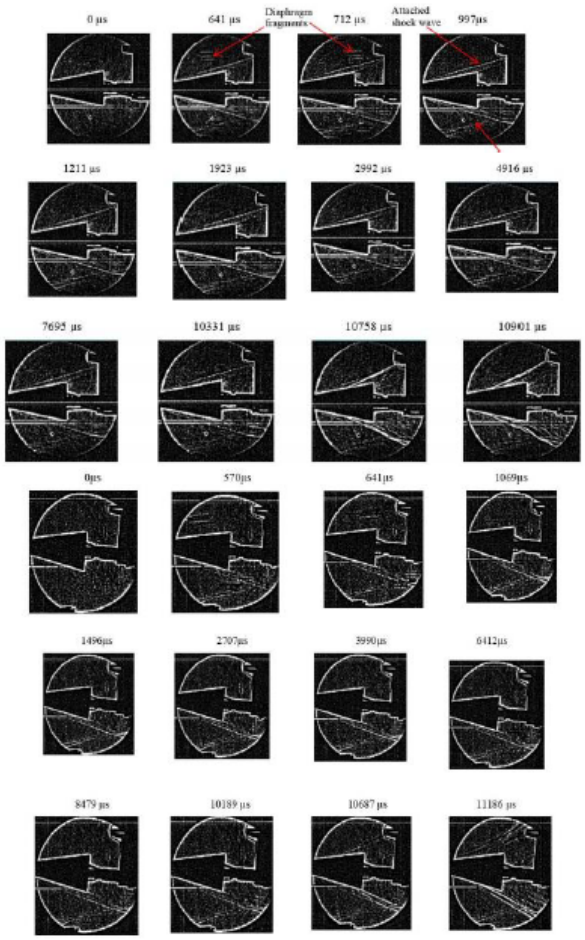

APPENDIX D: Block Diagram and Command Window of LabView